Energy Conversion and Management: X 2 (2019) 100011

Contents lists available at ScienceDirect

Energy Conversion and Management: X

journal homepage: www.journals.elsevier.com/energy-conversion-and-management-x

Analysis of technologies and potentials for heat pump-based process heat supply above 150 °C

B. Zühlsdorf[a,b,*], F. Bühler[a], M. Bantle[c], B. Elmegaard[a]

[a] Technical University of Denmark, Department of Mechanical Engineering, Nils Koppels Allé, Bygning 403, 2800 Kgs, Lyngby, Denmark
[b] Danish Technological Institute, Energy and Climate, Kongsvang Allé 29, 8000 Aarhus, Denmark
[c] SINTEF Energi AS, Department of Thermal Energy, 7465 Trondheim, Norway

ARTICLE INFO

Keywords:
Electrification
R-718
R-744
Reversed Brayton cycle
Process heat
Steam compression

ABSTRACT

The transition of the manufacturing industry towards carbon neutrality requires a reduction of the emissions from combustion for the supply of process heat. Heat pumps are an efficient alternative technology for supplying heat while improving the overall efficiency and shifting to potentially carbon neutral electricity. The state-of-the-art technology is limited to supply temperatures between 100 °C and 150 °C because of lower efficiency and component limitations. This paper has therefore analyzed two promising concepts for higher supply temperatures and found technically and economically feasible solutions for process heat supply of up to 280 °C. These solutions are using large-scale equipment from oil and gas industries for applications in energy-intensive industries. The suggested systems benefitted from the economy of scale and access to low electricity prices. The concepts outperformed a biogas-based solution, and they were competitive with biomass or natural gas systems with respect to economic performance. It was concluded that an electricity-based heat supply is possible for a wide range of industrial applications and accordingly represents an important contribution to fulfilling the objectives of lower climate impact of energy supply in industry.

1. Introduction

The combustion of fossil fuels for the supply of process heat is becoming unattractive due to increasing fuel costs and CO_2 emission. At the same time, the electricity production from renewable energy sources becomes cheaper [1] and the ratio between cost for electricity from renewables and of fossil fuels decreases [2]. The industry sector of the EU is expected to decrease its greenhouse gas emissions by at least 80 % compared to 1990 until 2050 [3]. Some countries have committed themselves to more thorough strategies. As an example, Denmark aims to be completely independent of fossil fuels by 2050 [4]. This will require significant and fundamental changes in the industry sector, and industries accordingly require alternatives to their current fossil fuel-based energy supply. As a result, the electrification of production processes receives a growing attention.

The *Deep Decarbonization Pathways Project* [5] analyzed different strategies for the practical transition of countries to low-carbon economies. It highlights the beneficial impacts of decarbonizing societies, while enabling growth in economy and population. In relation to the industry sector, improvements in energy efficiency and conservation as well as shifting to emission-free fuels are listed as requirements.

Bataille et al. [6] reviewed the technologies and pathways which enable industries to develop in line with the Paris Agreement [7]. It was outlined that new industrial facilities must be emission-free by 2035 to reach the targets defined in the Paris Agreement. The identified strategy included a general political commitment, followed by local incentives, such as carbon pricing or incentivizing energy efficiency measures, to enhance the market penetration of emission-free or negative emission technologies. The authors further outlined the necessity to bring near-commercial CO_2 emission-free technologies into industries and included heat pumps as alternatives for process heat supply for up to 250 °C.

McMillan et al. [8] analyzed the use of thermal energy in the industrial sector of the US and studied the possibilities to reduce the associated greenhouse gas (GHG) emissions. A large share of the GHG emissions of the industrial sector stemmed directly from fuel combustion for process heat supply and could be reduced by using CO_2 emission-free fuels as well as energy and material efficiency improvements.

The industry in Europe is highly heterogeneous. It represented 25 % of the final energy use in 2015 [9]. The heterogeneity of the industry and the variety of different production methods on a process level enables different degrees of process integration and requires a detailed

* Corresponding author at: Danish Technological Institute, Energy and Climate, Kongsvang Allé 29, 8000 Aarhus, Denmark.
E-mail addresses: bez@dti.dk (B. Zühlsdorf), fabuhl@mek.dtu.dk (F. Bühler), Michael.Bantle@sintef.no (M. Bantle), be@mek.dtu.dk (B. Elmegaard).

https://doi.org/10.1016/j.ecmx.2019.100011
Received 18 January 2019; Received in revised form 27 April 2019; Accepted 13 May 2019
Available online 25 May 2019

Nomenclature

Abbreviations

CEPCI	Chemical Engineering Plant Cost Index
GHG	Greenhouse gas
HP	Heat pump
HTHP	High temperature heat pump
HX	Heat exchanger
IC	Intercooler
IHX	Internal heat exchanger
TC	Turbocompressor

Variables

A	Area, m^2
c_{alt}	Specific cost per unit heat from alternative supply, €·MWh^{-1}
c_{el}	Specific cost per unit electricity, €·MWh^{-1}
c_h	Specific levelized cost of heat, €·MWh^{-1}
COP	Coefficient of performance, −
COP_{Lor}	Coefficient of performance for Lorenz cycle, −
COP_{R-718}	COP of R-718 multi-stage system, −
COP_{R-744}	COP of R-744 reversed Brayton cycle, −
C_P^0	Purchase cost for equipment at standard conditions, €
CF	Annual cash flow, €·$year^{-1}$
CF_{alt}	Annual income from replacing alternative heat supply, €·$year^{-1}$
CF_{el}	Annual cost for electricity consumption, €·$year^{-1}$
CRF	Capital recovery factor, $year^{-1}$
f_{CEPCI}	Factor to account for the year of the cost function, −
f_{BM}	Bare module factor, −
f_M	Material factor, −
f_P	Pressure factor, −
IRR	Internal rate of return, %
k_i	Factors in cost functions, −
NPV	Net present value, €
OH	Annual operating hours, h·$year^{-1}$
p	Pressure, bar
PBT	Simple payback time, years
$\dot{Q}$	Transferred heat rate, kW
$\dot{Q}_{sink}$	Heat rate supplied to sink, kW
$\bar{T}_{Sink}$	Thermodynamic average temperature of heat sink, K
$\bar{T}_{Source}$	Thermodynamic average temperature of heat source, K
TCI	Total capital investment, €
TCI_{spec}	Specific total capital investment, €
U	Heat transmission coefficient, W·m^{-2}·K^{-1}
$\dot{W}$	Power, kW
$\dot{W}_{comp}$	Compression power, kW
$\dot{W}_{exp}$	Expansion power, kW
X	Scaling parameter in cost functions, see Table 4
ΔT_{lm}	Logarithmic mean temperature difference, K
η_{gear}	Efficiency of gear, −
η_{Lor}	Lorenz efficiency, −
η_{motor}	Efficiency of motor, −

analysis to establish the optimal GHG emission pathways. On the other hand, electrification technologies, applicable to a wide range of industrial processes without requiring major modifications to existing infrastructure would ease the replacement of fossil fuel-based utility systems.

Electric-driven heat pumps have proven to be suitable for supplying process heat in a sustainable and effective way, while improving the overall energy efficiency. Wolf and Blesl [10] conducted numerical studies to quantify the contribution of industrial heat pumps with respect to the mitigation of climate change. Considering state-of-the-art equipment and CO_2 emissions from the German electricity generation mix of 2015, it was found, that reductions of 15 % of the final energy consumption and 17 % of the total energy-related CO_2 emissions could be obtained considering technical constraints only. These potentials reduced to 2.3 % and 4.2 %, respectively, under consideration of economic boundary conditions. A sensitivity analysis revealed a strong beneficial impact of decreasing electricity cost and decreasing investment cost on the profitability of heat pumps. The economically feasible reductions of GHG emission that are obtainable by heat pumps are however expected to increase due to the ongoing decarbonization of the energy sector and decreasing levelized cost of electricity of renewable electricity generation technologies, such as wind and photovoltaic [11]. The electrification is further incentivized by decreasing primary energy factors, which benefit the environmental evaluation of electricity-based heat supply [12].

Heat pumps with sufficient performances are available as state-of-the-art equipment for supply temperatures of up to 100 °C, while different projects demonstrated the technical feasibility of supply temperatures as high as 150 °C to 180 °C, [13,14]. Other studies [15,16] have shown that a relevant heat demand at higher temperatures exists. Among others, material constraints and equipment costs were identified as barriers for industrial high-temperature heat pumps (HTHP) [17]. Increasing the technically feasible supply temperatures of heat pump equipment would further increase the implementation potential and constitute a promising alternative for an efficient and CO_2 emission-free supply of process heat in industrial processes.

State-of-the-art equipment from other sectors, such as chemical processing, might enable the construction of heat pumps exceeding the limitations of heat pumps using equipment originally developed for refrigeration purposes. In order to evaluate these possibilities in more detail, the state of the art is reviewed and potential solutions for heat pump-based process heat supply above 150 °C are identified.

The objectives of this work are i) to demonstrate the techno-economic feasibility of constructing large-scale high-temperature heat pumps for process heat supply, ii) to estimate the environmental and economic potential of the technologies considering different energy supply scenarios in different case studies, and iii) to analyze the potential for applications in different industrial sectors including required actions to exploit this potential.

2. State of the art of heat pumps for supply temperatures above 150 °C

In the literature, different cycles were considered for the supply of process heat at high temperatures. The best cycle for a given application will depend on the framework conditions of the processes, namely the heat sink and source characteristics. In the following, two cycles are introduced and their limitations as well as possible promising applications are discussed. The two cycles that were chosen are a multi-stage cycle using R-718 (water) as refrigerant, which can be constructed as an open or closed system, and a reversed Brayton cycle using R-744 (CO_2) as refrigerant. Both refrigerants are natural refrigerants with a high acceptance in industrial applications.

2.1. Steam compression systems

Steam supply is an established technology for process heating purposes. The steam can be either injected directly into the process or it can be condensed and subcooled in heat exchangers to supply process heat. The direct steam injection corresponds to an open cycle, while the

alternative using the heat exchangers is a closed system. Central steam generation units have the advantage of large loads and the possibility to balance the time shift in the demand of different processes, which means extended utilization of the unit. It appears to be promising due to the high utilization of the equipment and low integration cost to consider heat pump-based steam generation systems as an alternative. Kang et al. [18] have reviewed the developments of steam generation heat pumps and analyzed different layouts. They indicated the necessity of further research on the comparison of different technologies using energy, exergy and economic analysis as well as on cascade and multi-stage cycles. They outlined furthermore the demand for research on the compressors for extending the applications to higher temperatures. Bless et al. [19] studied different possibilities for heat pump-based steam generation and outlined the high thermodynamic performances.

The heat pump performance is essentially influenced by the availability of heat sources. Heat sources at sufficiently high temperatures might be directly integrated, while heat sources from lower temperatures can be integrated by means of a bottom cycle. Kaida et al. [20] have analyzed the experimental performance of a system in which steam is generated by a bottom cycle and upgraded to higher pressures by turbocompressors, reaching supply temperatures of 165 °C. Lee et al. [21] studied the suitability of different working fluids for a heat pump, which can be used to produce low-pressure steam or operate as a bottom cycle for a cascade system.

Meroni et al. [22] compared different high-temperature cycles of a cascade heat pump for the generation of steam at 150 °C. The study considered a detailed design of the compressor and found that the direct compression of water in a two-stage cycle outperformed the closed loop cycles using different other working fluids.

Bühler et al. [23] presented a steam generation unit based on a central heat pump that consisted of bottom cycles, supplying heat to a central evaporator at 90 °C while integrating various heat sources, and a high-temperature multi-stage steam compression unit, which supplied steam at different pressure levels to the processes. The presented system had a COP of 1.95 and had the best thermodynamic and economic performance compared to other electrification scenarios that were using decentralized heat pumps and/or electrical heaters.

Various studies have furthermore focused on the analysis of compression equipment that is suitable for the compression of steam. Madsbøll et al. [24] developed a turbocompressor that is suitable to achieve a temperature lift in saturation temperatures of water of 25 K to 30 K at evaporation temperatures of 90 °C to 110 °C. Bantle et al. [25] studied the possibilities to utilize turbocompressors in superheated steam drying applications. Later, Bantle et al. [26] presented experimental tests of a single-stage turbocompressor cycle, which achieved a temperature lift of approximately 25 K. Most recently, Bantle et al. [27] presented an experimental study of a two-stage system. The developed technology was based on mass-produced turbocharger technology from automobile applications. The specific investment costs per unit of supplied heat of systems using this technology were expected to reach values as low as 200 €/kW. Zühlsdorf et al. [28] have shown that steam compressors based on this technology reach economically reasonable sizes for evaporation temperatures above 90 °C to 100 °C. Chamoun et al. [29,30] conducted experiments in a similar operating regime using a twin-screw compressor. While the performance was similar, higher investment cost were expected for the screw compressors. Larminat et al. [31] presented the development and experimental tests for a turbocompressor achieving a temperature lift between saturation temperatures of 90 °C and 130 °C.

These studies demonstrated the technical feasibility of steam compression equipment for supply temperatures of up to 150 °C to 160 °C, while it could be expected that higher temperatures can be achieved with similar equipment. Especially turbocompressors appear to be a promising solution, as they may potentially operate oil-free and

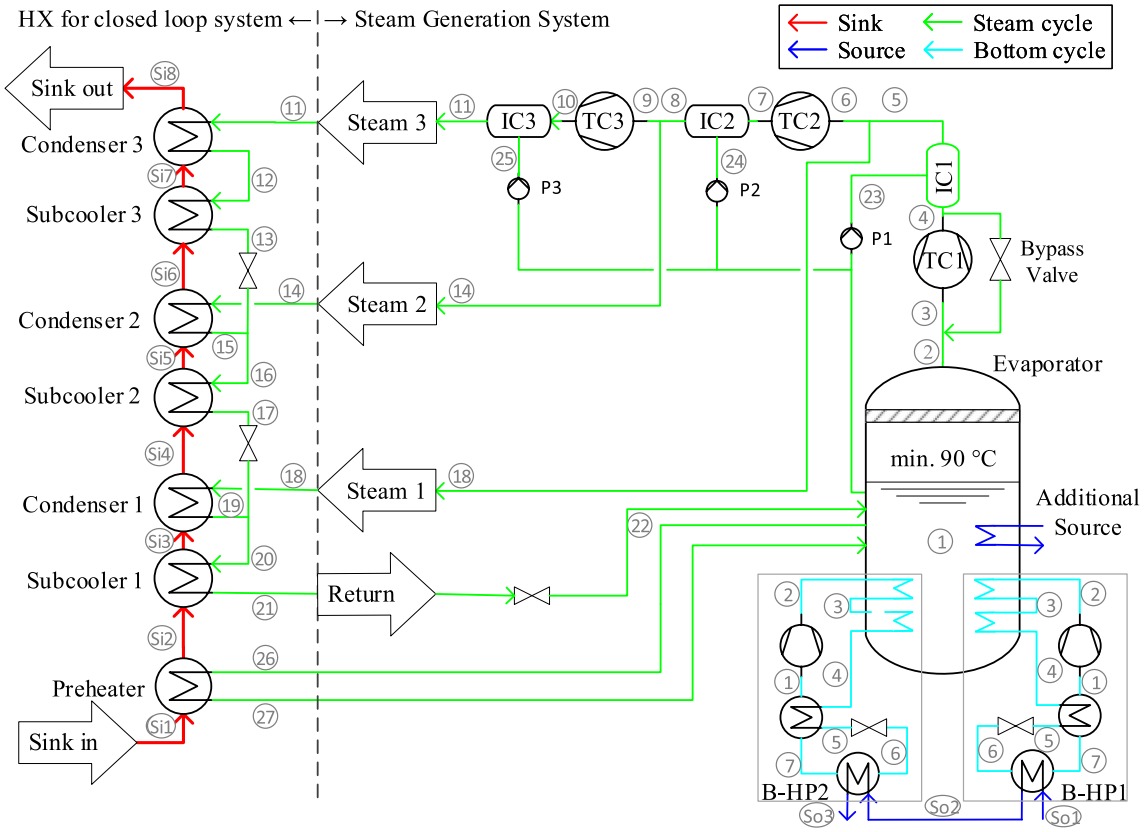

Fig. 1. Flow sheet of a cascade heat pump with a multi-stage R-718 cycle for steam generation or closed loop heat supply at different temperature levels (B-HP = Bottom heat pump, IC = Intercooler, P = Pump, TC = Turbocompressor).

therefore are not limited by current lubrication systems [14]. The obtained pressure ratios per compression stage that could be obtained by turbocompressors reached values of up to 3.5, which is consistent with the expectations from [32,33]. The supplied heat loads achieved in the experimental studies were in the order of up to 1 MW.

While steam compression shows a high efficiency for cases in which both the heat source and sink have relatively constant temperatures with a small glide, it implies inefficiencies when used in applications in which single phase fluids with a certain temperature glide are heated. In such applications, vapor compression cycles using zeotropic mixture [34] or gas cycles [35] might show improved efficiency in cases with larger temperature glides, in which e.g., a single-phase fluid is heated.

2.2. Reversed Brayton cycle

Angelino and Invernizzi [35] reviewed the prospects of reversed Brayton cycles and considered them as a viable alternative for heat supply at high temperatures. Fu and Gundersen [36] presented a method for integrating reversed Brayton cycles in industrial sites and outlined the potential of exploiting the temperature glides in the application.

General Electrics (GE, previously ALSTOM Power) suggested a reversed Brayton heat pump using R-744 (CO_2) in supercritical conditions to be used in a pumped heat electricity storage system [37–39]. R-744 is a natural working fluid with a high industrial acceptance. The storage medium was molten salt in liquid conditions that was heated from 290 °C to 565 °C and stored in tanks. The heat pump used turbocompressors with maximum discharge temperatures that allowed heating the molten salt up to 480 °C, while the remaining temperature lift up to 565 °C was achieved with an electric heater. The heat pump cycle included furthermore an expander that was mounted on the same shaft as the compressor. Considering a heat source at 60 °C, a COP of 1.3 was reported in which only a heat pump was used to supply heat at 465 °C and a combined COP of 1.2, when the temperature was boosted to 565 °C with an electrical heater. During the discharge periods, the molten salt from the hot tank was used to drive a conventional steam power plant.

The heat pump was designed for high-temperature and large-scale applications and utilized large-scale equipment from chemical processes. The maximum scale was constrained by a size of commercially available compressors of 40 MW electrical power. The maximum compressor discharge temperature was found to be high enough to supply a process stream of up to 480 °C while high pressures of up to 140 bar were expected to be feasible. The heat exchangers were assumed to be shell and tube heat exchangers. This highlights that compressors can be found, which are capable of high temperature levels (> 400 °C) and thereby exceed the supply temperatures achieved by compression equipment originating from the refrigeration industry. It may furthermore be noted, that the specific cost of such equipment is decreasing at large capacities, indicating that especially large-scale applications might result in economically feasible solutions.

3. Methods

In the following, the general assumptions for the thermodynamic and economic modelling of the cascade multi-stage steam compression system and the reversed Brayton cycle are introduced. Subsequently, possible applications for large-scale high-temperature heat pumps are determined and case studies for a specific evaluation of the technologies are defined.

3.1. Design of considered heat pump systems

3.1.1. Vapor compression heat pumps using R-718

This work considers a cascade heat pump that was based on the system described [23] and visualized in Fig. 1. The high temperature cycle is a three-stage cycle that supplies heat to the process stream at three different pressure levels and receives subcooled liquid at the temperature of the evaporator from the process. The bottom cycle can consist of one or more cycles in parallel which integrate different heat sources and supply the central evaporator. Heat sources that are available at sufficient temperature can be integrated directly. The cycle was designed to obtain a minimum temperature of 90 °C in the evaporator in order to keep the volume flow rates of the compressors for R-718 at a reasonable level [28]. If a large enough amount of heat is available at higher temperatures, the temperature of the evaporator is increased and no bottom heat pumps are required. In case that bottom heat pumps were required, the evaporator temperature was limited to 125 °C, as this could be covered with state-of-the-art equipment by using e.g., R-600 (butane) [40].

The high-temperature cycle consists of a multi-stage vapor compression cycle using R-718 as working fluid. After each compression stage the steam is desuperheated to 10 K above its saturation temperature by injecting saturated liquid from the evaporator. The three-stage system was designed to achieve maximum supply temperatures of around 210 °C at an evaporation temperature of 90 °C, while it could be extended to higher temperatures by adding more stages in the same manner or increasing the evaporator pressure. The system can be designed as an open system in which the steam is directly injected into the process streams or as a closed system in which the steam is condensed and subcooled before returned to the central evaporator.

In the closed system, the liquid of the high temperature stages is subcooled to the saturation temperature of the next-lowest stage and mixed with the saturated liquid from this stage. Based on the presented literature [32,33], a maximum pressure ratio of 3.5 was assumed and if a higher temperature lift was required, an additional compression stage was considered. The amount of steam supplied to the process at each stage is defined by the application and the system is dimensioned accordingly. All heat demand that occurred below the evaporator temperature was directly covered with liquid condensate, which was returned to the evaporator at subcooled conditions. If the heat demand was required at temperatures that were too high for cooling the liquid to the evaporator temperature, it was flashed into the evaporator tank.

Table 1 summarizes the assumed component efficiencies for the numerical modelling. The isentropic efficiency and the maximum pressure ratio were chosen in accordance with [27,28,32]. No pressure drops and heat losses within the piping and the heat exchangers were considered for the simulations. In a closed system, the liquid was sufficiently subcooled to the temperature of the evaporator, while the liquid feed was accordingly heated by an auxiliary heat pump for an open system. The evaporator was assumed to be ideally mixed, while no pumping power was considered.

The thermodynamic performance of the steam cycle was evaluated by its $COP_{R\text{-}718}$. The $COP_{R\text{-}718}$ was defined as the ratio of the supplied heat $\dot{Q}_{sink}$ to the total power consumed $\dot{W}_{total}$. The total power consumption comprised the sum of the compressor power $\sum \dot{W}_{comp}$ of the different compressors from the bottom and the high-temperature cycle as well as the power of all pumps $\sum \dot{W}_{pump}$ under consideration of an efficiency for the motor η_{motor} and the gear η_{gear}. The supplied heat load $\dot{Q}_{sink}$ assumed that the steam is in both cases subcooled to the evaporator temperature and completely used for process heating purposes. If heat was covered by using the saturated liquid from the evaporator,

Table 1
Modelling assumptions for steam compression heat pump.

Isentropic efficiency compressor	75 %
Efficiency of pumps	90 %
Efficiency of motor η_{motor}	95 %
Efficiency of gear η_{gear}	95 %
Maximum pressure ratio per stage	3.5
Remaining superheat after liquid injection	10 K

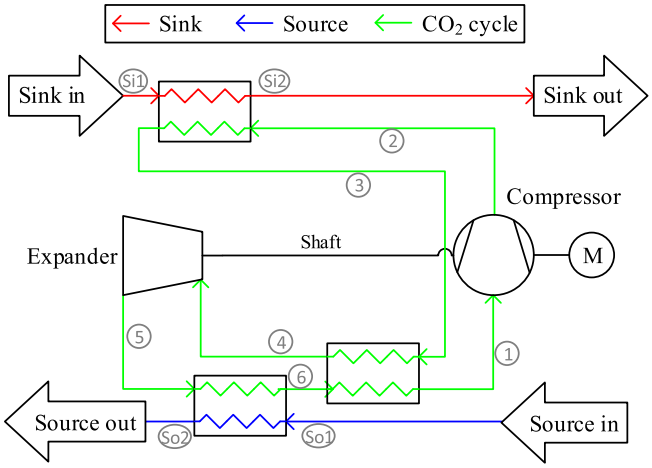

Fig. 2. Flow sheet of reversed Brayton cycle.

this was considered as well.

$$\mathrm{COP}_{\mathrm{R-718}} = \frac{\sum \dot{Q}_{\mathrm{sink}}}{\dot{W}_{\mathrm{total}}/(\eta_{\mathrm{motor}}\eta_{\mathrm{gear}})} \tag{1}$$

The bottom heat pump cycles were modelled as described in [41,42]. The compressor was modelled with an isentropic efficiency and the expansion process assumed to be isenthalpic. The pressure levels and the subcooling were defined by minimum pinch point temperature differences. The transferred heat in the internal heat exchanger was maximized, as this yielded the maximum COP, while a minimum pinch point temperature difference was respected. The efficiencies for the compressor, the gear and the drive were assumed as for the high-temperature cycle. The heat exchangers were modelled with separate sections in which the refrigerant was in either liquid, gas or two-phase conditions. It was however assumed that the evaporator and the superheater as well as the desuperheater and condenser were manufactured as one component. Considering that all thermodynamic state points were defined, the mass flow rates were determined by mass and energy balances in order to meet the process heat demands.

3.1.2. Reversed Brayton cycle

Fig. 2 shows the layout of the considered reversed Brayton cycle. The compressor was also in this case a turbocompressor. It was mounted on the same shaft as a turbine that recovers the expansion work. The recovery of expansion work appeared promising due to the high pressure ratios and since expansion occurred in the gas phase. Recovering the expansion work was not considered in the multi-stage R-718 cycle, as the thermodynamic potential was smaller and since the expansion was located within the two-phase zone. Further, an internal heat exchanger was considered to cool the working fluid subsequent to the gas cooler while heating the stream in front of the compressor.

Table 2 summarizes the modelling inputs. The isentropic efficiencies of the turbomachinery are dependent on the specific working conditions and the capacity, while conservative estimates based on e.g., [35], were assumed for this study. No pressure drops or heat losses from the piping or the heat exchangers were considered. The pressure levels were optimized with respect to a maximum COP, while the pressure was constrained to a maximum of 140 bar. The outlet conditions of the turbine were a design parameter and they were optimized to be at least 5 K above the corresponding saturation temperature. The definition of the turbine outlet temperature indirectly determined the pinch point temperature difference and thereby the size of the internal heat exchanger. The mass flow rate was determined by the heat load required by the process.

Table 2
Modelling assumptions for reversed Brayton cycle.

Isentropic efficiency compressor	75 %
Isentropic efficiency turbine	75 %
Efficiency of motor η_{motor}	95 %
Efficiency of gear η_{gear}	95 %

The $\mathrm{COP}_{\mathrm{R\text{-}744}}$ was determined as the ratio of the supplied heat $\dot{Q}_{\mathrm{sink}}$ to the difference of the compressor power $\dot{W}_{\mathrm{comp}}$ and the expander power $\dot{W}_{\mathrm{exp}}$ under consideration of an efficiency for the motor η_{motor} and the gear η_{gear}.

$$\mathrm{COP}_{\mathrm{R-744}} = \frac{\dot{Q}_{\mathrm{sink}}}{(\dot{W}_{\mathrm{comp}} - \dot{W}_{\mathrm{exp}})/(\eta_{\mathrm{motor}}\eta_{\mathrm{gear}})} \tag{2}$$

3.2. Thermodynamic evaluation

In order to evaluate the efficiency of the cycles, the COPs were related to the maximum achievable COP of a theoretical cycle. The Lorenz cycle [43] is a theoretical cycle with an isentropic compression and expansion process and heat transfer at the thermodynamic average temperatures [44] of the heat source $\bar{T}_{\mathrm{Source}}$ and the heat sink $\bar{T}_{\mathrm{Sink}}$. The performance of the Lorenz cycle is described by the $\mathrm{COP}_{\mathrm{Lor}}$.

$$\mathrm{COP}_{\mathrm{Lor}} = \frac{\bar{T}_{\mathrm{Sink}}}{\bar{T}_{\mathrm{Sink}} - \bar{T}_{\mathrm{Source}}} \tag{3}$$

The Lorenz efficiency η_{Lor} describes the efficiency of the respective cycle by relating the COP to the Lorenz $\mathrm{COP}_{\mathrm{Lor}}$.

$$\eta_{\mathrm{Lor}} = \frac{\mathrm{COP}}{\mathrm{COP}_{\mathrm{Lor}}} \tag{4}$$

3.3. Economic evaluation

In order to evaluate the economic performance, the investment costs as well as the operating costs need to be calculated. For the estimation of the investment costs, the component dimensions of the main components were determined before the capital costs were estimated using correlations. The capital costs were subsequently compared to the operating cost under consideration of the time value of the money for different representative cost scenarios.

3.3.1. Component dimensioning

The estimation of the capital cost of the equipment requires an estimation of the component dimensions for the main components of the system. The component costs were estimated based on parameters describing the components capacity or dimensions. For some of the components, such as the compressors, turbines and drives, the capacity was described by the power, which was directly available from the thermodynamic calculations. The capital costs for heat exchangers was determined based on their area.

The relation between the required area A and the transferred heat $\dot{Q}$ for a heat exchanger in which two streams of constant capacities are exchanging heat was described by Eq. (5) [44]. The heat exchangers were discretized in sufficiently small parts of equal heat transfer to allow the assumption of constant capacities.

$$\dot{Q} = UA\Delta T_{\mathrm{lm}} \tag{5}$$

The UA-value was determined by the logarithmic mean temperature difference ΔT_{lm}. In order to determine the area A from the UA-value, the heat transmission coefficient U was estimated. The heat transmission coefficient U considers the heat transfer coefficients on both sides of the heat exchangers. Dependent on the design of the heat exchangers and the involved fluids, a range of heat transfer coefficients can be achieved for technically feasible and economically reasonable heat exchanger designs. The heat transfer coefficients considered in this study were estimated based on the experience-based values from [45]. Table 3 summarizes the heat transfer coefficients, the components and

Table 3
Assumptions for the heat exchanger selection and dimensioning dependent on the involved process streams.

Side 1	Side 2	Heat exchanger type	Minimum pinch point temperature difference, K	Heat transfer coefficient, U $Wm^{-2}K^{-1}$
Gas (e.g., air)	Working fluid (liquid)	Shell & tube HX	7.5	42.5
	Working fluid (gaseous)	Shell & tube HX	7.5	40.0
	Working fluid (condensing)	Shell & tube HX	7.5	42.5
	Working fluid (evaporating)	Shell & tube HX	7.5	42.5
Liquid (e.g., water)	Working fluid (liquid)	Shell & tube HX	5.0	750.0
	Working fluid (gaseous)	Shell & tube HX	5.0	42.5
	Working fluid (condensing)	Shell & tube HX	5.0	1000.0
	Working fluid (evaporating)	Shell & tube HX	5.0	1000.0
Working fluid (evaporating)	Working fluid (condensing)	Evaporator vessel with internal coils	5.0	1250.0
Working fluid (gaseous, high pressure)	Liquid (e.g., thermal oil)	Shell & tube HX	7.5	150.0
	Working fluid (gaseous)	Shell & tube HX	7.5	70.0

the minimum pinch point temperature differences that were used in this study depending on the involved streams.

3.3.2. Component cost estimation

The purchase cost for the components in base conditions, meaning basic material at standard operating conditions without auxiliary equipment, C_P^0, was determined by a cost function as described in Eq. (6) [46,47]. The parameters that were used for these cost functions are summarized in Table 4 and were taken from the same literature.

$$\log(C_P^0) = k_1 + k_2\log(X) + k_3(\log(X))^2 \tag{6}$$

The bare module cost of the equipment C_{BM} includes both the direct and indirect cost related to the component. The cost for auxiliary materials, labor and engineering is summarized by the bare module factor f_{BM}. The additional cost for the design of the equipment in different material and to operate at increased pressures are estimated by the factors f_M and f_P, as defined in [46,47]. A pressure factor $f_P = 1.2$ was assumed for the construction of the heat exchangers at the high pressure side of the R-744 cycle.

$$C_{BM} = f_{BM} f_P f_M f_{CEPCI} C_P^0 \tag{7}$$

As the cost functions were reported in different years, the cost estimations were converted to values corresponding to the year 2017 by the factor f_{CEPCI}, which was based on the Chemical Engineering Plant Cost Index (CEPCI).

Based on the bare module cost of the components, the total component costs can be estimated by considering a factor of 18 %, accounting for possible contingencies and fees [46]. The costs for integrating the unit on site and retrofitting an existing plant, an additional factor of 15 % was considered, yielding the total capital investment cost TCI. In order to compare the TCI of different solutions, the specific total capital investment was expressed as in relation to the supplied heat load TCI_{spec}. To account for the non-energy related operation and maintenance costs, an additional 20 % of the TCI was used as a one-time payment.

3.3.3. Economic performance indicators

The net present value NPV was chosen for the evaluation of the economic performance of the different solutions, as it is an indicator that considers the entire lifetime of the plant [44,47,48]. The NPV considers both the total capital investment cost TCI and the summed cash flows for each year CF. The cash flows were expected to be constant throughout the lifetime and were converted to their time value at the time of the investment by the capital recovery factor CRF. The CRF considered an effective interest rate of 5 % and a lifetime of the plant of 20 years.

$$\mathrm{NPV} = -\mathrm{TCI} + \frac{\sum \mathrm{CF}}{\mathrm{CRF}} = -\mathrm{TCI} + \frac{\mathrm{CF_{alt}} - \mathrm{CF_{el}}}{\mathrm{CRF}} \tag{8}$$

The levelized specific cost of heat c_h was considered as another measure for the comparison of the alternatives. It relates the investment cost corresponding to one year of operation TCI·CRF and annual operating cost due to consumption of electricity or another fuel $\sum \mathrm{CF}$ to the annually supplied heat $\mathrm{OH}\cdot\sum \dot{Q}_{sink}$.

$$c_h = \frac{\mathrm{TCI}\cdot\mathrm{CRF}}{\mathrm{OH}\cdot\sum \dot{Q}_{sink}} + \frac{\sum \mathrm{CF}}{\mathrm{OH}\cdot\sum \dot{Q}_{sink}} \tag{9}$$

The simple payback time PBT was introduced as a measure for the estimation of the uncertainties associated with the investment, by determining the period which is required until the profit compensated the total capital investment without considering the time value of the cash flows. The payback time is however insufficient for the evaluation of the profitability of the investment, as it only considers part of investments lifetime [44,47,48].

$$\mathrm{PBT} = \frac{\mathrm{TCI}}{\mathrm{CF_{alt}} - \mathrm{CF_{el}}} \tag{10}$$

As an additional indicator the internal rate of return IRR [44] was used, which is defined as the interest rate at which the NPV of the investment equals zero.

The sum of the annual cash flows represents the annual savings that would result from substituting the existing energy utility with the suggested system. The cash flow resulting from the electricity consumption in the considered scenario CF_{el} was determined by the sum of the consumed power $\sum \dot{W}$, the annual operating hours OH and the specific electricity cost c_{el}. The cash flow describing the savings for substituting the alternative heat supply CF_{alt} was defined by the amount of the supplied heat $\sum \dot{Q}_{sink}$, the operating hours OH and the specific cost for the alternative heat supply c_{alt}.

$$\mathrm{CF_{el}} = c_{el}\,\mathrm{OH}\sum \dot{W} \tag{11}$$

$$\mathrm{CF_{alt}} = c_{alt}\,\mathrm{OH}\sum \dot{Q}_{sink} \tag{12}$$

Both the specific cost for the alternative heat supply and the electricity consumption are effective costs, meaning that they are including the net price, additional fees and taxes and in case of the alternative heat supply also the boiler efficiency. The following section discusses the different scenarios and presents the considered costs.

3.3.4. Scenarios for the economic and environmental evaluation of the case studies

This section defines economic and environmental scenarios for the evaluation of the case studies, which are summarized in Table 5. The heat pumps can be based on electricity supply from the grid or from

Table 4
Parameters for estimation of component capital cost.

Component	Scaling parameter X	Range	k_1	k_2	k_3	Year	f_{BM}	Ref.
Centrifugal/reciprocating compressors	Fluid power	450 kW – 3000 kW	2.2897	1.3604	−0.1027	2001	2.8	[46]
Drive (electric, totally enclosed)	Shaft power	75 kW–2600 kW	1.9560	1.7142	−0.2282	2001	1.5	[46]
Evaporator plain vessel	Volume	1 m^3 – 800 m^3	3.5970	0.2163	0.0934	2004	3.0	[47]
Internal coils in evaporator tank	Area	1 m^2 – 8000 m^2	3.2195	0.3743	0.046	2004	1.0	[47]
Screw compressors	Fluid power	10 kW – 1000 kW	3.4756	0.6814	$-8 \cdot 10^{-6}$	2004	2.2	[47]
Shell & tube heat exchanger	Area	10 m^2 – 900 m^2	3.2476	0.2264	0.0953	2004	3.2	[47]
Turbine (radial)	Fluid power	100 kW–1500 kW	2.2476	1.4965	−0.1618	2001	3.5	[46]

own renewable electricity production facilities. The electricity prices and the associated CO_2 emissions are varying according to the local electricity markets, electricity mix and taxes. The analysis was based on data from three countries, which were selected as exemplifying scenarios. Germany was chosen as it has a large and diverse industrial sector and a large share of fossil fuel-based electricity production, while Denmark has a large share of renewable electricity from wind and Norway from hydro. The share of electricity production from wind, solar and hydro accounted for 97.6 % in Norway and for 46.6 % in Denmark in 2016 [49]. The cost scenarios that were selected for these countries corresponded to the most favorable conditions, which are typically limited to customers with consumption in the range of energy-intensive industries. It may be noted that customers with lower electricity demands may be paying higher prices. The selection of the ambitious electricity prices was however based on the assumption, that the industries with access to the lowest electricity tariffs will be the first ones for which the installation of heat pumps will become beneficial. It was furthermore expected that the installation of the suggested heat pump systems increases the electricity consumption to a considerable extent, which may give access to lower electricity tariffs.

Philibert [11] emphasizes the possibility for energy-intensive industries to invest directly in renewable electricity production facilities. An additional scenario was added. It was assumed that only electricity from wind and solar is accepted and that the industry itself acquires and operates the electricity generation. It is expected that the levelized cost of electricity from renewables can become as low as 30 €/MWh, depending on the location and combination of different technologies [1,11]. Based on [50,51] and assuming Danish conditions, the levelized cost of electricity in 2020 is expected to range from 30 €/MWh for onshore wind energy to 47 €/MWh for offshore wind, with nearshore wind energy and large photovoltaic at 41 €/MWh. Additional costs are expected for storage facilities and measures to operate the local electricity grid. For this study, an average levelized cost of electricity of 40 €/MWh was assumed, with a potential range of 30 €/MWh to 50 €/MWh.

The heat pump technologies were evaluated for the aforementioned scenarios and were compared to different technologies. As potential alternative technologies, an electrical boiler and different combustion-based boilers were considered. Natural gas, biogas and biomass were considered as fuels for the combustion-based boilers. The specific cost including taxes for natural gas was 27.7 €/MWh for Norway [52,53], 28.7 €/MWh for Denmark [54–56] and 33.1 €/MWh for Germany [2]. For this study, a range of 28 €/MWh to 33 €/MWh was assumed. The installation of a natural gas boiler was associated with a specific investment cost of 103 €/kW of heating capacity [56]. The specific cost for biomass was assumed to be in the range of 64 €/MWh for normal biogas and 75 €/MWh for upgraded biogas [57]. The investment cost for the gas boiler for biogas was assumed to be the same as for natural gas. The market price of biomass was assumed to be in the range of 28 €/MWh for wood chips and 33 €/MWh for wood in Denmark in 2020 [58]. The investment cost for biomass boilers including storage facilities was assumed as 800 €/kW of heating capacity [56].

The specific scenarios are summarized in Table 5. It includes the specific fuel cost, specific CO_2 emissions and the potential technologies. The specific CO_2 emissions of natural gas were assumed as 0.204 t/MWh [59], while they were assumed to be zero for biogas and biomass. The combustion of biomass and biogas might however be subject to a NO_x-tax as it is in Denmark [54].

3.4. Evaluation of the application potential of heat pump-based process heating at high temperatures

In order to identify industries and processes where high temperature heat pumps can have a promising application potential, industrial sectors were evaluated as a basis for the selection of case studies for a deeper analysis of the technical and economic potential.

The evaluation criteria for promising applications were industrial processes where (i) heat is required at temperatures between 150 °C and 450 °C, (ii) heat is typically supplied from external sources (e.g., steam from boilers, combustion heat) and not internally (e.g., from exothermic reactions or through process integration), (iii) the heat demand is high (above 1 MW) and (iv) heat is required continuously and with a high number of annual operating hours.

3.4.1. Identification of promising industrial sectors

Several studies analyzed the industrial process heat demand and excess heat including the temperature ranges on industry sector level for different countries. Naegler et al. [60] quantified the industrial heat

Table 5
Considered fuels and potential technologies for 2020 conditions.

Fuel		Fuel price incl. taxes, €/MWh			Specific CO_2 emissions, kg/MWh	Potential technologies
		Chosen value	Lower range	Upper range		
Electricity	Denmark [55–57]	63.1	–	–	461	- Reversed Brayton cycle
	Germany [2]	52.1	–	–	624	- Steam Compression cycle
	Norway [53,54]	36.1	–	–	570	- Electric boiler, η = 0.95, TCI_{spec} = 210 €/kW
	Renewable [1,11]	40.0	30.0	50.0	0	
Natural Gas [55–57]		31.0	28.0	34.0	204	- Gas boiler, η = 0.9, TCI_{spec} = 103 €/kW
Biogas [46,56,57]		69.5	64.0	75.0	0	
Biomass [2,46,57]		30.5	28.0	33.0	0	- Biomass boiler, η = 0.9, TCI_{spec} = 800 €/kW

demand on a European level. Based on data for Germany the share of process heat demand in the range of 100 °C to 500 °C was found to be highest in the chemical, food, paper and construction industry, where the share was between 20 % and 70 % of the total heat demand of the respective sector. While the share of process heat demand between 100 °C and 500 °C was approximately 20 % of the industrial heat demand in the largest industrial heat user countries, it was above 30 % in Sweden, Finland and Portugal.

Rehfeldt et al. [61] also analyzed industrial processes in Europe using bottom-up estimates and similarly found that the pulp and paper, food and beverages and chemical industry have the highest heating demands in the range of 100 °C and 500 °C, but also the processing of non-metallic minerals was found to have a high heat demand in this range. The distribution of process heat demand among European countries was found to vary. On average 40 % of process heat is required above 500 °C, the heating demand between 100 °C and 500 °C was 30 % but in some countries (e.g., Finland, Sweden, U.K. and Austria) it was considerably higher. The processes accounting for the major share of the heat demand in the temperature range between 200 °C and 500 °C were secondary aluminum production and rolling/extruding of aluminum, flat glass, gypsum and ethylene production. A majority of the energy use in food, beverage, pulp and paper industries was found in the temperature range between 100 °C and 200 °C.

McKenna and Norman [62] analyzed heating demands for industrial sectors and the recovery potential for excess heat for the UK. The pulp and paper, food and drink and chemical industry sectors were found to have the majority of its heat demand between 100 °C and 500 °C. The heating demand in this temperature range accounted for 160 PJ, out of a total heat demand of 788 PJ. The recovery potential of heat was estimated to be between 37 PJ and 73 PJ per year [63].

Arpagaus et al. [14] analyzed different heating demands based on literature data, to identify the potentials for heat pumps with supply temperatures up to 140 °C. For Germany the potential of process heat which is coverable by heat pumps with sink temperatures between 80 °C and 140 °C was estimated to be 337 PJ. The main processes for high-temperature heat pump application were identified in drying, pasteurizing, sterilization, evaporation and distillation processes.

The pulp and paper industry has a large potential for energy efficiency, where heat recovery and integration presents the largest CO_2 mitigation potential at the lowest specific costs [64]. The use of heat pumps is an important approach in obtaining a high level of energy efficiency, however the process temperatures are typically below 150 °C where heat pump technologies are available [65]. This sector is therefore not further considered in this study for the use of HTHP.

Based on these findings, the following industrial sectors were identified as sectors, in which the presented technologies were expected to potentially be able to increase the temperature limits for process heat supply to above 150 °C, while yielding economically feasible performances:

- Chemical and petrochemical industry
- Ferrous and non-ferrous metal industry
- Non-metallic minerals industry
- Food and beverage industry

3.4.2. Case studies

Two case studies were defined to analyze the energetic, environmental and economic performance in more detail. The case studies were chosen representing possible applications from the aforementioned industries. Based on the case study results, the potential for further applications in these industries is discussed.

3.4.2.1. Case study of alumina production. The aluminum production has a high energy intensity, which results in an accordingly high rate of CO_2 equivalent emissions [66] and accounts for a high share of the final product costs [67]. A large share of the energy is consumed during the refining of bauxite to alumina, which is a basic material for the aluminum production [68]. The Bayer process is the most established process for the refining of bauxite and the largest share of the energy is required as heat for preheating and digesting the bauxite, while the maximum temperatures vary between 140 °C and 280 °C, depending on the quality of the bauxite, the utilized equipment and various other factors [67].

The heat for preheating and digesting the bauxite slurry can be supplied by steam or by single-phase fluid, e.g., molten salt or a thermal oil [69–71]. Steam can be injected directly, while the single-phase fluids require heat exchangers for indirect heat exchange. The latter results in larger temperature differences but higher energy efficiencies [72].

As the entire process is energy-intensive, there is a high availability of excess heat at sufficient temperatures, which could potentially be utilized as a heat source of a heat pump. A suitable heat source could e.g., be the exhaust air from the calcination stage [73].

For the evaluation and comparison of the heat pump technologies, a representative case study was defined, corresponding to potential conditions as described by the aforementioned literature. It was assumed that heat is supplied to a stream of constant heat capacity flow rate, e.g., thermal oil or a molten salt, which is heated from 140 °C to 280 °C, while heat is taken from excess heat from another on-site process between 110 °C and 60 °C. The required heat load was defined as 50 MW, as this corresponds to typical plant sizes and approximately to the largest commercially available compressors for the reversed Brayton cycle [37]. The mass flow rate of the source was determined by the system COP. The annual operating hours were assumed as 8000 h/year.

3.4.2.2. Case study of a spray drying facility. Spray drying facilities in the food industry are typically accounting for a large portion of the energy use of the sector and represent some of the highest process temperatures. Spray dryers are furthermore often in the range of several megawatts capacity and often operate throughout the year. This makes them a promising application for a heat pump-based process heat supply. In spray dryers, the liquid is atomized and sprayed into a drying chamber with heated air [74]. The droplets of food move with the heated air and the water evaporates.

In this study, we considered a spray drying facility based on the milk production site for which Bühler et al. [75] conducted an energy, exergy and advanced exergy analysis. Zühlsdorf et al. [34] studied the integration of heat pumps with zeotropic mixtures for the same spray drying facility. They presented a heat pump solution to preheat the drying air to 120 °C, which decreases the natural gas consumption by 36 %. Bühler et al. [23] compared further different strategies for the design of a fully electrified production system. After the integration of direct heat recovery, the inlet air with a mass flow rate of 54.9 kg/s and a humidity of 6.43 g/kg had to be preheated from 64 °C to 210 °C, while the outlet air with a mass flow rate of 64.3 kg/s and a humidity of 28.88 g/kg at a temperature of 50 °C could be used as heat source. The amount of heat recovered from the heat source, and accordingly the outlet temperature, were determined by the system COP. The annual operating hours were assumed to be 7000 h/year.

4. Results

The Brayton cycle and the steam compression unit were evaluated for two case studies under consideration of the different economic and environmental boundary conditions. The main technical parameters of the two concepts for the two case studies are presented in the following, before the economic analysis is presented and the potentials of the technologies for other industries are discussed.

4.1. Technical concepts for the case studies

4.1.1. Multi-stage steam compression cycle (R-718)

The steam compression cycles for both applications were designed with 3 compression stages. The two low-pressure stages were chosen with a pressure ratio of 3.2, while the pressure ratio of the third stage was 2.84 for the alumina production case study and 3.03 for the spray dryer case study. The overall COP was 1.9 for both cases, which corresponds to a Lorenz efficiency of 49 %.

Fig. 3 shows the temperature-heat diagram and Fig. 4 the logarithmic pressure-enthalpy diagram for the steam compression cycle for the alumina production case. The heat sink inlet temperature was 140 °C, and the evaporator temperature was chosen to be 125 °C, as it could be supplied by a bottom heat pump using butane (R-600) [40]. The evaporator pressure was 2.3 bar and the condensing pressures of stage 1, 2 and 3 were 7.4 bar, 23.8 bar and 67.5 bar and the compressor outlet temperatures 302 °C, 355 °C and 397 °C, respectively. The compressors were of 5.8 MW, 5.6 MW and 3.4 MW shaft power capacity. The COP of the R-718 steam compression cycle was 3.0.

The two bottom heat pumps were single stage heat pumps with an internal heat exchanger using R-600. The capacities of the heat pumps were chosen to recover an equal amount of heat of each 12.8 MW from the heat source while supplying a total amount of 34.9 MW to the evaporator of the high temperature cycle. The first heat pump cycle operated with an evaporation pressure of 9.6 bar and had a COP of 4.2, while the second bottom heat pump had an evaporation pressure of 5.3 bar and a COP of 2.9. The condenser pressure was 26.3 bar in both cases.

Both bottom cycles were designed with a maximum internal heat exchange, as this yielded the maximum COP. This did however also result in a large amount of desuperheating, which might imply larger volume flow rates, a larger pressure drop and a large temperature gradient in the desuperheater.

Fig. 5 shows the temperature-heat-diagram for the multistage steam compression cycle for the spray dryer case. In this case, the sink inlet temperature was below 90 °C, which was defined as the minimum evaporation temperature with respect to reasonable compressor volume flow rates [28]. This enabled that the first part of the stream could be preheated by direct heat transfer using liquid from the evaporator holdup. The evaporation pressure was 0.7 bar, while the pressure in the condensers were 2.2 bar, 7.2 bar and 21.8 bar. The compressors had a shaft capacity of 0.8 MW, 0.6 MW and 0.4 MW and outlet temperatures of 257 °C, 301 °C and 344 °C for stage 1, 2 and 3, respectively.

Also for the spray dryer case, two bottom heat pump cycles with an internal heat exchanger using R-600 were chosen. In this case, the heat source was moist air and the first heat pump was designed to recover the heat until the dew point of 31 °C while the second heat pump cycle recovered the remaining heat including the condensing heat of the moist air. The first heat pump had an evaporation pressure of 2.3 bar and recovered 1.3 MW with a COP of 3.1. The second cycle had an evaporation pressure of 1.6 bar and recovered 3.0 MW from the condensing moist air with a COP of 2.7. Both bottom cycles had a condenser pressure of 13.7 bar. Due to the flexibility of designing the bottom heat pump cycles according to the heat source characteristics, the condensing heat of the moist air could be efficiently recovered.

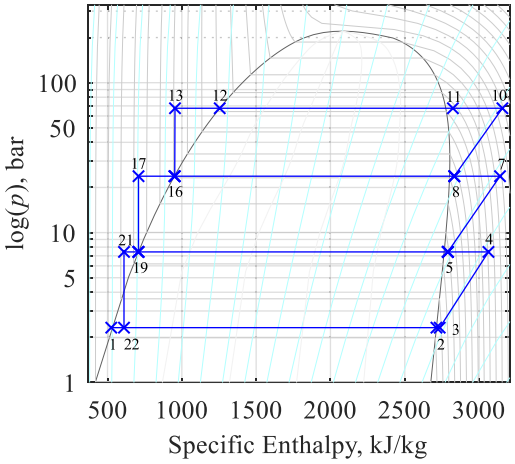

Fig. 4. Logarithmic pressure-enthalpy-diagram for the R-718 top cycle of the heat pump for the alumina production case study with selected state point numbers indicated.

4.1.2. Reversed Brayton cycle (R-744)

Fig. 6 shows the temperature-heat-diagram and Fig. 7 the temperature-entropy-diagram for the reversed Brayton cycle for the boundary conditions of the alumina production case study. The optimal pressures were 40.7 bar at the low pressure side and 140 bar at the high pressure side, which corresponds to a pressure ratio of 3.4. The outlet temperature of the compressor was 290 °C, The COP of the cycle reached 1.72, which was slightly lower than 1.92 as obtained for the steam compression cycle. The cycle performance corresponds to a Lorenz efficiency of 44 %.

It may be noted that the temperature profiles of the heat exchangers were matching well in all heat exchangers, indicating a small amount of irreversibility during heat transfer. The pinch point in the heat source heat exchanger occurred at the source inlet, indicating that a higher

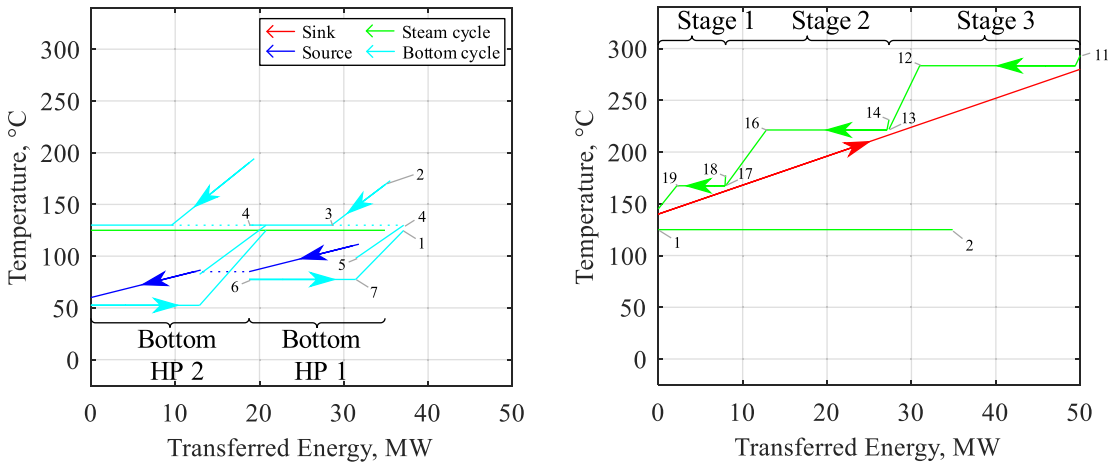

Fig. 3. Temperature-heat-diagram for the bottom cycles using R-600 (left) and the multi-stage top cycle using R–718 (right) for the alumina production case study. Selected state point numbers are shown for the bottom HP 1 and for the multi-stage cycle.

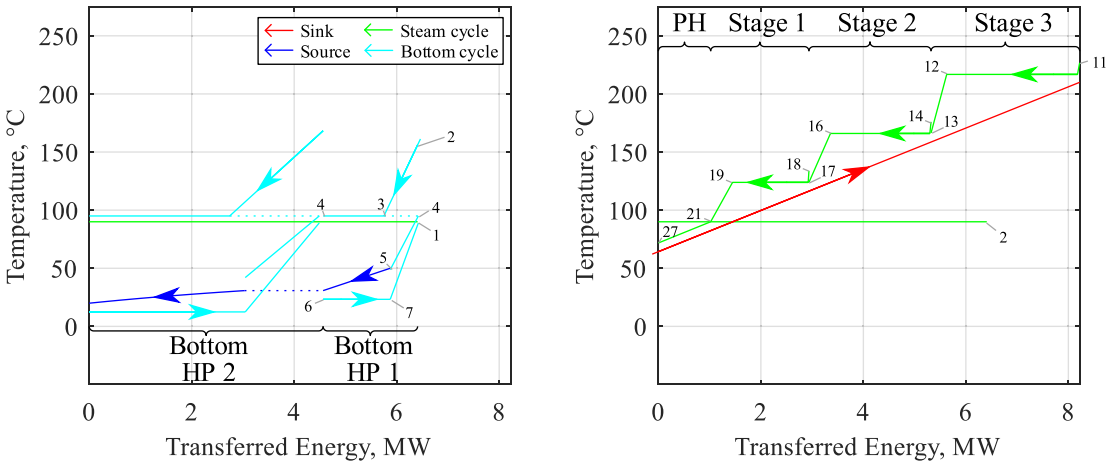

Fig. 5. Temperature-heat-diagram for the bottom cycles using R-600 (left) and the multi-stage top cycle using R–718 (right) for the spray dryer case study. Selected state point numbers are shown for the bottom HP 1 and for the multi-stage cycle.

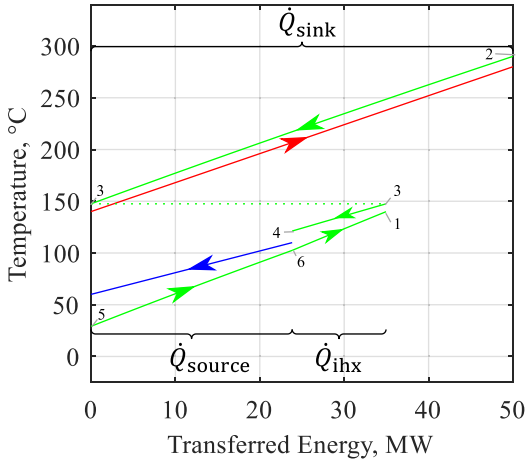

Fig. 6. Temperature-heat-diagram for the reversed Brayton cycle using R-744 for the alumina production case study.

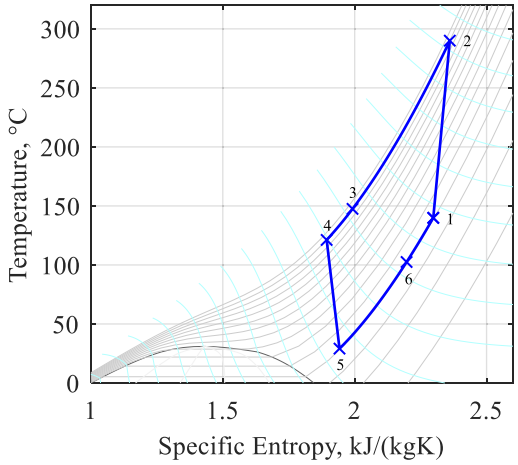

Fig. 7. Temperature-entropy state diagram for the reversed Brayton cycle using R-744 for the alumina production case study.

inlet temperature would allow to design the system with a higher low pressure or respectively, that the heat source could be cooled down further, resulting in an increased heat exchanger area but without compromising the thermodynamic performance.

Fig. 8 shows the temperature-heat-diagram for the case of the spray dryer. The reversed Brayton cycle reached a COP of 1.61 and a Lorenz efficiency of 40 % while operating with a low pressure of 25.2 bar, a high pressure of 72.0 bar and accordingly a pressure ratio of 2.9. The outlet temperature of the compressor was 218 °C.

The temperature-heat-diagram shows a mismatch between the streams in the heat exchangers. This results inevitably in irreversibility and decreased overall performance. In the heat sink, the pinch point occurs at the heat sink outlet, indicating that the thermodynamic performance could be improved by a lower outlet temperature or, respectively, that the heat sink inlet temperature could be higher without having to increase the pressures. On the source side, the inlet temperature of the working fluid lies below 0 °C, while the heat source outlet temperature was around 25 °C. While the characteristic of the condensing moist air is well exploited by the bottom heat pumps of the cascade multi-stage system, there remains some potential for improvements in the case of the reversed Brayton cycle.

An overview of all state points for both cycles and both cases is given in the Appendix.

4.2. Economic analysis of case studies

The suggested systems were furthermore evaluated with respect to their economic performance by determining the investment cost and comparing this to the operating cost. Table 6 shows an overview of the total capital investment TCI for the two systems for both cases. For the

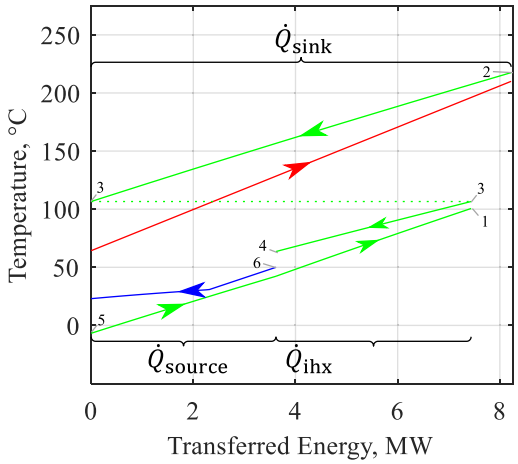

Fig. 8. Temperature-heat-diagram for the reversed Brayton cycle using R-744 for the spray dryer case study.

Table 6
Total capital investment incl. maintenance cost for both cases and both systems incl. subsystems.

Unit	Alumina production		Spray Dryer	
	TCI Mio. €	TCI_{spec} €/kW	TCI Mio. €	TCI_{spec} €/kW
Total cascade multi-stage system	**47.34**	**946**	**16.42**	**1997**
- Top multi-stage cycle (R-718)	22.86		9.30	
- Bottom cycle 1 (R-600)	11.19		2.16	
- Bottom cycle 2 (R-600)	13.29		4.95	
Reversed Brayton system (R-744)	**48.32**	**966**	**15.35**	**1868**

alumina case, the TCI of the cascade multi-stage system was 47 Mio. €, and thereby approximately as expensive as the reversed Brayton system, which had a TCI of 48 Mio. €. For the spray dryer case, the cascade multi-stage system had a TCI of 16 Mio. €, while the reversed Brayton system had a slightly lower TCI of 15 Mio. €. It may furthermore be noted that the specific investment cost were considerably lower for a capacity of 50 MW supplied heat compared to 8.2 MW supplied heat, which corresponds to the expectations with respect to the economy of scale of Aga et al. [37]. While it is expected that the decreased specific investment cost resulted mainly from the upscaling, it may be mentioned, that the specific area of the heat sink heat exchanger was significantly smaller for the alumina case than for the spray dryer case, as the heat transfer coefficient was almost four times larger when heating thermal oil instead of air.

The specific levelized heat generation cost c_h as summarized in Fig. 9 were used to compare the investment cost to the operating cost. The diagram is based on the cost assumptions as introduced in Table 5. The levelized cost was divided into the shares corresponding to fuel consumption and investment. The specific fuel cost for renewable electricity, natural gas, biogas and biomass was specified with a certain range, which is included in the diagram by means of black bars. In order to visualize the impact of a tax on CO_2 emissions, an exemplifying tariff of 50 €/t of CO_2 was assumed and added in the diagram.

The specific levelized cost of heat for the alumina production case varied for both heat pump systems between 45 €/MWh for Denmark and 31 €/MWh for Norway, disregarding any cost for CO_2 emissions. Considering electricity from own renewable electricity facilities, the levelized cost of heat is expected to be between 29 €/MWh and 39 €/MWh for both systems for the alumina case. For the case of the spray dryer, the specific cost of heat were between 9 €/MWh and 12 €/MWh higher, mainly due to higher specific investment cost and a worse COP of the reversed Brayton system.

The investment cost contributed by approximately 10 €/MWh for both systems in case of the alumina production case study, while it reached 20 €/MWh to 22 €/MWh for the spray dryer case study.

An electrical boiler in combination with renewable electricity was considered as an alternative electricity-based heat supply technology. The levelized specific cost of heat was 51 €/MWh with a possible variation between 40 €/MWh and 64 €/MWh. The heat pump systems are accordingly able to compensate the increased investment in terms of levelized cost.

Combustion-based boilers using natural gas, biogas and biomass were considered as further alternatives. The specific investment cost for the gas boilers was minor, while it accounted for approximately 11 €/MWh for the biomass boiler. The levelized cost accumulated 34 €/MWh to 40 €/MWh for natural gas, 73 €/MWh to 85 €/MWh for biogas and 42 €/MWh to 48 €/MWh for biomass, while a potential tax on CO_2 emissions of 50 €/t would yield and additional cost of approximately 10 €/MWh for natural gas.

It may accordingly be summarized that the heat pump systems showed performances which were competitive with natural gas boilers and biomass boilers, when electricity was obtained at low cost. The two heat pump systems were competitive with natural gas boilers without tax on CO_2 emissions, when the electricity was obtained at costs of up to 50 €/MWh in the alumina production case and of up to approximately 35 €/MWh in the spray dryer case. The heat pump systems based on renewable electricity could operate at same levelized cost of heat as a natural gas boiler in the spray dryer case, when a tax of 46 €/t and 35 €/t of CO_2 were assumed for the reversed Brayton system and the multi-stage system, respectively.

Table 7 summarizes the COP, the total capital investment TCI, the net present value NPV, the simple payback times PBT and the internal rate of return IRR for a comparison of the heat pump systems to a combustion-based heat supply. For the alumina production case the

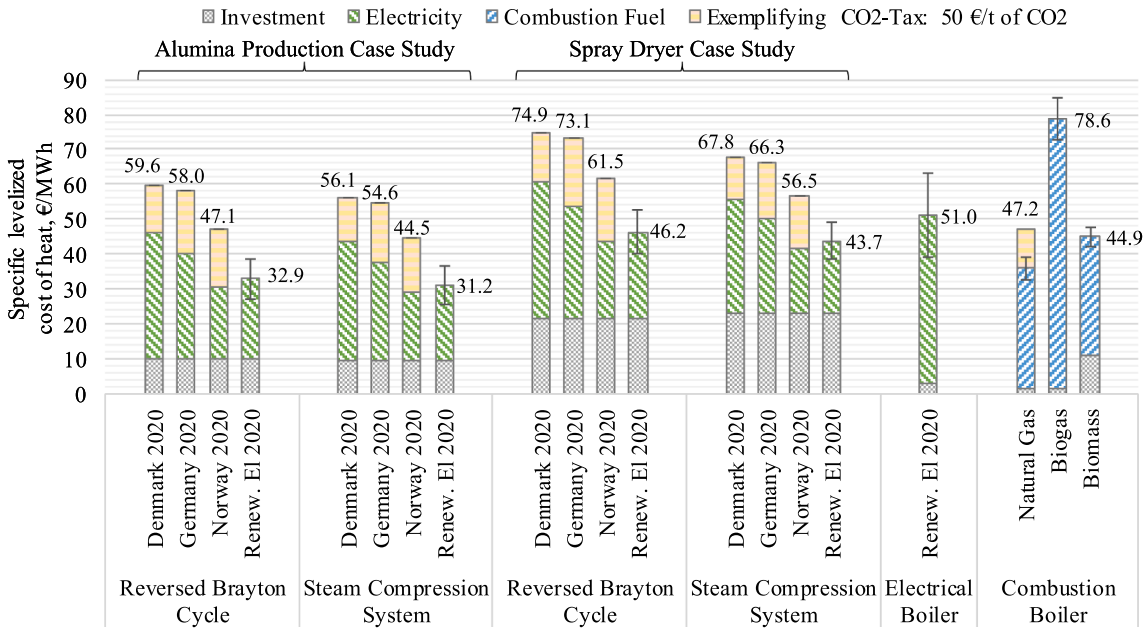

Fig. 9. Specific levelized cost of heat c_h for both case studies including the reversed Brayton cycle, the multi-stage steam compression cycle, an electrical boiler and combustion-based boiler using natural gas, biogas and biomass. The cost scenarios are as defined in Table 5 while the ranges for the cost for electricity from renewables, natural gas, biogas and biomass are indicated by the black bars.

Table 7
Total capital investment TCI, net present value NPV, simple payback time PBT and internal rate of return IRR for both cases and cycles for selected scenarios as defined in Table 5 and assuming specific cost for natural gas of 28.7 €/MWh in Denmark, 33.1 €/MWh in Germany and 27.7 €/MWh in Norway and no taxes for CO_2 emissions. For the comparisons to renewable electricity, the specific cost for natural gas, biogas and biomass were assumed according to the average value as given in Table 5.

	Alumina production		Spray dryer	
	Cascade multi-stage system	Reversed Brayton cycle	Cascade multi-stage system	Reversed Brayton cycle
Coefficient of performance COP, -	1.92	1.72	1.92	1.61
Total capital investment TCI, Mio. €	47.3	48.3	16.4	15.4
Net present value NPV, Mio. €				
Denmark 2020 – NG	−44.8	−64.7	−16.1	−19.5
Germany 2020 – NG	8.05	−8.5	−8.5	−11.1
Norway 2020 – NG	19.6	7.8	−6.8	−8.3
Renewable el 2020 – NG	27.8	14.8	−5.6	−7.4
Renewable el 2020 – BG	241.0	228.1	25.0	23.2
Renewable el 2020 – BM	72.8	59.9	0.8	−1.0
Payback time PBT, years				
Denmark 2020 – NG	–	–	–	–
Germany 2020 – NG	10.7	15.1	25.8	45.4
Norway 2020 – NG	8.8	10.7	21.3	27.2
Renewable el 2020 – NG	7.9	9.5	19.0	24.2
Renewable el 2020 – BG	2.1	2.2	4.9	5.0
Renewable el 2020 – BM	4.9	5.6	11.9	13.3
Internal rate of return IRR, %				
Denmark 2020 – NG	–	–	–	–
Germany 2020 – NG	6.9	2.8	–	–
Norway 2020 – NG	9.5	6.8	–	–
Renewable el 2020 – NG	11.2	8.4	0.5	–
Renewable el 2020 – BG	48.9	45.9	19.7	19.6
Renewable el 2020 – BM	19.8	17.2	5.6	4.2

heat pump systems were outperforming biogas, biomass and natural gas when based on renewable facilities, and were competitive with natural gas when considering Norwegian conditions. For the spray dryer case the heat pump systems became feasible when based on renewable facilities and compared to biogas and biomass, but they were outperformed by natural gas based systems in all scenarios considering no taxes on CO_2 emissions.

The simple payback times PBT shown in Table 7 are below 5 years if the electricity is obtained from own renewable resources and the alternative is biogas in both cases and are below 6 years when compared to biomass in the alumina production case. In the alumina case the reversed Brayton cycle has a PBT of 10 years and the steam compression unit of 8 years when own renewable-based electricity and natural gas consumption from the grid is assumed. The IRR for the reversed Brayton cycle reached 8 % and for the cascade multi-stage system 11 %. These values might be accepted, considering that the investment improves the overall efficiency and constitutes the central utility system, which is associated to corresponding low uncertainties.

The economic results indicated a strong dependency on the specific cost for electricity c_{el} and for the alternative heat supply c_{alt}. In order to analyze this dependency in more detail, a parameter study was conducted. Figs. 10 and 11 show the net present value NPV of the reversed Brayton cycle and the steam compression unit for a variation of the specific cost between 20 €/MWh and 100 €/MWh for the alumina production case study. Additionally, the specific levelized cost of heat for natural gas, biomass and biogas are indicated on the axes. The same information is shown for the steam compression cycle in Fig. 11.

Considering the cheapest cost for the alternative fuel for a natural gas-based combustion process of 33 €/MWh, the NPVs of both technologies become positive for specific electricity costs lower than 40 €/MWh. Presuming that the aim is a fully carbon neutral solution, natural gas is eliminated as a potential alternative and the remaining options considered here are biomass or biogas. The cheapest levelized cost of heat from biomass is around 42 €/MWh. Considering this benchmark, the electrification of the processes using the suggested technologies becomes the preferred choice for electricity generation cost lower than 53 €/MWh. Compared to biogas, the heat pump-based process heat supply constitutes the most favorable solution in all scenarios, incl. “Germany 2020” and “Denmark 2020”.

The replacement of a natural gas-based combustion process with specific CO_2 emissions of 0.204 tons/MWh corresponds to an abatement of 90,800 tons of CO_2 per year in the case of the alumina production and to 13,100 tons of CO_2 per year in the case of the spray dryer. Replacing oil or coal based heating utilities results in accordingly higher emission reductions. The impact of increased prices for CO_2 emission certificates on the economic performance was demonstrated in Fig. 9 and may be additionally derived from Figs. 10 and 11 by adding the costs to the alternative fuel costs.

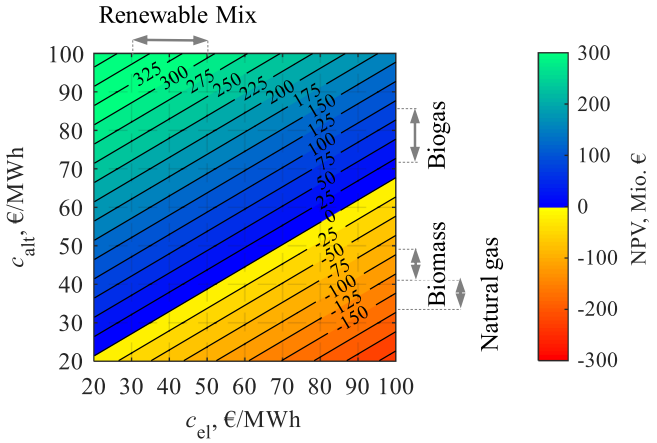

Fig. 10. Net present value NPV for a variation of the specific cost for electricity c_{el} and the alternative heat generation c_{alt} for the reversed Brayton cycle in the alumina production case study with an indication of the specific cost of different energy utilities.

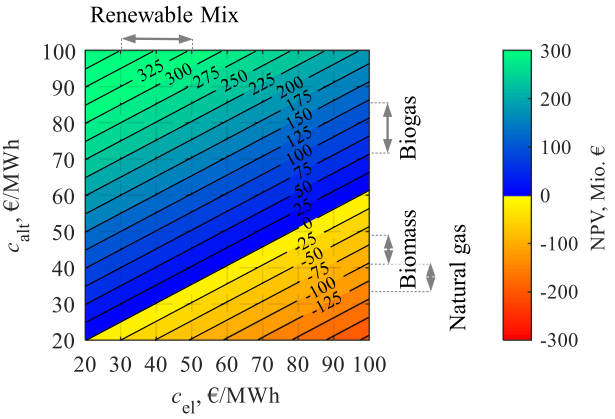

Fig. 11. Net present value NPV for a variation of the specific cost for electricity c_{el} and the alternative heat generation c_{alt} for the steam compression cycle in the alumina production case study with an indication of the specific cost of different energy utilities.

4.3. Identification of additional industrial processes as potential applications

The two case studies demonstrated the thermodynamic, economic and environmental performance of the presented technologies. They indicated that the performance of the heat pumps is strongly dependent on application and thereby subject to site specific parameters. The estimation of the potential does accordingly require inclusion of a detailed energy analysis of the existing process including a reevaluation of design parameters, which were decided considering a fuel-based heat supply.

It can be assumed that similar performances could be obtained for other processes, if adjustments of the production processes are accepted, while heat pump-based solutions are infeasible or unfavorable in other processes. In the following an analysis of the potential of the presented technologies for process heat supply in the range of 100 °C to 400 °C is shown for processes of other industrial sectors.

4.3.1. Chemical and petrochemical industry

The chemical and petrochemical industry in Europe is very diverse, with the German one being the largest. In Germany 25 % of the industrial energy use is associated with this industry sector [9]. The basic chemical industry is characterized by energy intense processes and large operation units, such as the production of ammonia, chlorine, ethylene and polymers. Other chemical industries produce for instance pesticides, paints, soaps, detergents and fibers. Some processes, such as steam crackers, require high temperatures and pressures while others receive the process heat from exothermic reactions, such as reactors. The largest potential for heat pump integration is found in distillation, evaporation, drying and heating processes, which often take place at temperatures between 100 °C and 500 °C [61]. Applications are for example the production of soda ash, where process temperatures of around 160 °C to 230 °C are required in the calcination process, where CO_2 and water are removed. While the main processes for the production of polymers are often exothermic, some process steps require heating. The production of polyamides requires pre-heating and heating in the range of 110 °C to 270 °C [76]. Polysulfones and polycarbonates further require process heat in the magnitude of 6.8 MWh and 3.6 MWh per ton respectively [77]. Process heat is required at temperatures between 120 °C and 300 °C for distillation, reactors, separators and dryers.

Heat pumps were suggested to be integrated for heat supply in hydrogen production processes [78,79] and significant improvements in overall performance were found. The heat pump required for the concept from [78] was required to deliver heat of up to 330 °C while receiving heat at around 265 °C. Almahdi et al. [79] suggested a cascade heat pump operating at even higher temperatures between 290 °C and around 670 °C.

Oil and gas refineries might be another promising application as it comprises energy-intensive processes with heat demands between 250 °C and 400 °C. Nemet et al. [80] performed a heat integration study for an oil refinery, where for one part of a factory a heating demand of more than 4 MW in the temperature range of 350 °C to 400 °C and 3 MW of heat requirement between 250 °C and 350 °C were found. At the same time, cooling of more than 4 MW is required between ambient and 130 °C. The HTHP using the reversed Brayton cycle could be suitable for this application. Oil refineries are however large and complex sites, where total site analyses are required to find the optimal integration strategies.

4.3.2. Ferrous and non-ferrous metal industry

The ferrous and non-ferrous metal industry comprise highly energy-intensive processes [66] and account for 21 % of the energy use in the European industry [9]. Most of the heat is however required at temperatures above 1000 °C and thereby above the techno-economic limitations of heat pumps. The high-temperature processes typically reject excess heat that can be used to cover other processes on site, which limits the potential for heat pump applications. The case study of the bauxite production was a pre-processing step in the aluminum production and locally it is independent of the actual aluminum production. It did however outline the possibility to reduce the overall environmental impact of the metal industry. Further processes in the ferrous and non-ferrous metal industry are in the temperature range between 100 °C and 400 °C. These might not be coverable by excess heat from other processes. Examples of these processes are in the post-processing (e.g., extruding, rolling) of copper and aluminum. In rolling processes, the materials are heated in ovens to temperatures between 350 °C and 510 °C. During the rolling process itself cooling of the rolls and materials take place [81].

4.3.3. Non-metallic mineral industry

The non-metallic mineral industry in Europe has a variety of products, such as cement, bricks, glass and ceramics. It accounted for 12 % of the energy use in the European industry [9]. The main processes take place in dryers and furnaces. While furnaces reach temperatures above 1200 °C, some of the heat is required at lower temperatures. In furnaces for ceramics around 10 % of the process heat demand is required below 500 °C [82]. The drying processes often aim at removing water and preheating the materials. In the production of asphalt the aggregate is dried and heated to temperatures above 200 °C using directly fired rotary dyers [83]. Spray dryers are used in the ceramic industry to remove water from the mud [84]. In the production of bricks and tiles, tunnel dryers are used for the formed materials where drying temperatures above 180 °C are required [85]. The moist air from the dryer is expelled at around 50 °C and latent and sensible heat can be recovered. While some of the available excess heat from the dryers could be used directly in the processes or is supplied from other process steps, e.g., the furnaces, high temperature heat pumps could be used to increase energy efficiency in some cases [85]. The process heat is usually added through direct combustion of natural gas or fuel oil to the processes.

4.3.4. Food and beverage industry

The food industry in Europe accounts for 11 % of the final industrial energy use [49] and includes industries such as meat and dairy processing, breweries and sugar production. The main processes in the food industry consist of pasteurization, sterilization, cooking, evaporation and drying. These processes usually take place below 120 °C. Drying processes however often require temperatures between 150 °C and 250 °C. They are used for many products, such as dairy, fruits, vegetables and beverages. They are also used in other industries in the production of dyestuffs, pigments and pharmaceuticals [86]. An estimated 25,000 spray dryers are commercially in operation worldwide

[86]. In 2016 the EU-28 produced a total of 2.8 million tons of milk powder. Special applications, e.g., found in production of bread, biscuits and cakes, require process temperatures above 170 °C for frying, drying and baking processes. The production of oil and fats has also high process temperatures for the refining and deodorization of the oils. The stripping of the oil, for instance, which removes volatile compounds, requires high temperature (> 200 °C) and pressure process steam, which is injected to the oils. Another example of an energy-intensive drying process is the drying of sugar beets. Superheated steam drying is state-of-the-art and yields promising efficiencies. It may be possible to improve further by using heat pumps, which may be similar to the configurations presented in this paper [87].

5. Discussion

5.1. Process modifications

The example of the alumina production from bauxite indicated that there is a certain freedom for the design of the process with respect to its heat supply. Considering that the heat for preheating and digesting the bauxite is transferred indirectly, the pinch point temperature difference can be chosen as a design parameter. This pinch point temperature difference describes the tradeoff among an increased heat exchanger area requirement at lower temperature differences compared to a decreased efficiency of the steam supply system for higher temperature differences [69–71]. The impact on the efficiency of the steam utility depends on the technology chosen for the heat supply. In conventional combustion-based steam generators, this impact is rather low, while it has a strong impact on the performance of heat pump-based steam generation systems. While pinch point temperature differences of 50 K to 70 K were accepted for conventional systems, values in the order of 10 K and accordingly larger heat exchanger areas are expected from an economic optimization considering heat pump-based steam generation. The results indicated that an additional temperature difference of 40 K to 60 K constitutes a vital impact on the profitability of the heat pumps.

In the case of the spray dryer, it was found that the temperature profiles did not match well. This resulted in a limited thermodynamic performance. The case study was based on a system layout which was already optimized without considering the possibility of a high-temperature heat pump. A simultaneous optimization of the layout considering the possibility of such high temperature heat pumps might result in more favorable conditions.

Based on these examples it can be concluded that a re-evaluation of process parameters that were selected based on combustion-based heat supply technologies are necessary and might be required for the design of an overall profitable solution. Furthermore, it is recommended to ensure that the most cost-effective energy efficiency measures are implemented before the heat pump systems are designed and integrated.

5.2. Flexibility in the design of the two studied concepts

Each process shows specific peculiarities and requires a case specific design of the heat pump solution as well as an analysis of the process parameters. For some processes, specific parameters might however not be adjustable and further process specific peculiarities occur. The spray dryer case involved e.g., moist air with a dew point around 31 °C as heat source. The reversed Brayton cycle had a limited performance due to the temperature profile mismatch in both the heat source and the sink, while the steam compression could be flexibly adjusted to the peculiarities of the process.

5.3. Technical assumptions

The isentropic efficiency for the compressors was assumed as 75 % while an additional efficiency for the drive and the gear of 95 % for each was considered. These efficiencies were conservative estimations and it was expected that these can be achieved or exceeded using state-of-the-art equipment, which might be adjusted to the specific application. The pinch point temperature differences were estimated smaller than for combustion-based systems but in a common range for heat pump systems. Increases in economic performance might be obtainable through a numerical optimization of the temperature differences. This would however require fixed economic boundary conditions and yield case specific results, which was outside the scope of this study. The study assumed furthermore no pressure drops and no heat losses, as this is subject to more detailed engineering. It is however expected that the impact of the pressure drops will be minor for properly designed systems and that the heat losses may be compensated by measures of reasonable economic extent.

The heat exchangers were assumed to be shell and tube heat exchangers, as these were proven technology for these applications and were considered by potential manufacturers [37]. Benefits in economic performance and aspects such as space requirements might however be obtained by selecting another heat exchanger type, such as printed circuit heat exchangers [88].

The limitations that were defined for the compression equipment exceeded the limitations that are typical for conventional heat pump systems [14] but they were in accordance with the values for equipment utilized e.g., in the oil and gas industry, which could potentially be used for these applications as well [37]. The pressure ratios for the R-718 cycle were assumed to be relatively high, which enabled a low number of compression stages but might imply challenges for the compressor design. The allowable pressure ratio and the number of stages might accordingly be optimized in a more detailed economic analysis.

One of the aspects that contributed to the choice of the studied systems was the state of the art of potential components. By the time of the publication, no publicly available documentation of demonstrations in full or lab scale could be found for any of the presented systems at the considered operating conditions. Aga et al. [37] do however emphasize, that the system is based on components that are commercially available and tested for the considered operating conditions and scales, while the reversed Brayton cycle is a known system as used in e.g., cryogenics. The multi-stage compression system used steam, which is widely used and a proven technology as utility system. Special requirements occur for the compressor, due to the high compressor outlet temperatures. Suitable equipment can however be found in oil and gas industries, while the operating requirements might be simplified by introducing more compression stages. It may accordingly be concluded that the Technology Readiness Level of both technologies in the suggested configurations and for the given applications is relatively low, while the conditions are promising to enable a fast development and up-scaling.

5.4. Uncertainties in the cost estimations

Some heat exchanger equipment was larger than the range for which the cost functions were developed and validated. It is expected that such heat exchanger equipment can be manufactured. The form of the cost functions is based on experiences from scaling equipment in general and it was therefore concluded that the estimates are still acceptable for equipment that is larger than the validated range. The estimates are however subject to increased uncertainties that would have to be analyzed during more detailed engineering.

It was furthermore indicated, that process modifications might potentially be required to enable optimal overall performances. The cost associated with such modifications is however dependent on the case-specific boundary conditions and to be considered accordingly in more detailed case studies.

The cost for operation and maintenance of the heat pump systems is expected to be higher than for boilers. A reliable evaluation of the operation and maintenance cost would however require a detailed

analysis of both the complete existing and the complete heat pump-based system and is therefore as well recommended for further, more detailed studies.

5.5. Cost of biomass and natural gas

The comparisons used the combustion of biomass and natural gas as benchmark scenarios. These resources are however limited and their prices are therefore affected by availability. Considering that coal and oil are eliminated as acceptable alternatives for combustion processes, the demand for the remaining alternatives will increase. The high-temperature processes will be prioritized, resulting in an increasing scarcity of these resources and thereby in increasing prices. The effective heat generation price for natural gas-based combustions is furthermore subject to political measures, such as the EU Emission Trading System, which might imply additional cost associated to emitting CO_2. These mechanisms are expected to result in the market becoming more beneficial for electricity-based solutions, but they are difficult to quantify and therefore they were omitted from the current study.

In the scenarios in which the heat pump-based solutions had the lowest NPVs, namely “Germany 2020” and “Denmark 2020”, the taxes for electricity consumption were higher than for natural gas. Considering the increasing awareness of the climate impact of fossil fuels and the increasing share of renewables in the electricity generation, it may be expected to change.

5.6. Acceptance of long payback periods

The presented technologies constitute a large investment, which typically requires low uncertainties to gain acceptance. The payback time was introduced as a measure to evaluate the uncertainties associated with the investment, as it describes the time span in which the investment is amortized. The accepted payback times depend on the uncertainties as well as on further factors, such as an increased plant competitiveness which might result from the investment.

Henrickson [89] studied different energy efficiency measures under consideration of the current economic situation, meaning developments of costs of fuels and bauxite, as well as of the product. He outlined the large contribution of energy to the operational expenditures and indicated that this will become even more dominating in the future. Based on this, Henrickson [89] concludes that longer payback times are accepted in the context of an ongoing modernization focusing on energy efficiency improvements, as such measures are resulting in an improved long term competitiveness.

The development of the energy costs constitutes one of the most uncertain assumptions in the economic evaluation. A general trend of decreasing cost for electricity generation from renewables and increasing cost for the combustion of fossil fuels, due to its environmental impact and decreasing availability, is expected [51], but not guaranteed. The exact development of costs is subject to political measures and market developments.

5.7. Acquisition and operation of own utility production

Philibert [11] outlined the possibility to acquire own renewable electricity utilities, which results not only in low but also stable electricity prices. The levelized cost of electricity from renewables was found to typically lie below the market prices. Owning both the electricity generation as well as the electricity consumption might furthermore enable the possibility to more effectively control the electricity consumption in accordance with its availability. The considered costs were assumed to be effective levelized costs, excluding cost for operation and control of the electricity system. The obtainable levelized cost of electricity depends furthermore on the approach to handle the variations in electricity supply. The variations might be compensated by local electricity storage or by the electricity grid, which in turn might be associated to a certain cost. It is also possible to choose a larger heat pump capacity in combination with thermal storages to obtain the possibility to vary the electricity consumption according to variable electricity input. The optimal combination of these measures is determined by case specific boundary conditions and subject to more detailed engineering.

Many industrial sites, especially large ones, generate their own heat in boilers, which are often coupled with gas turbines to produce electricity. The use of gas turbines in combination with a combined heat production is often seen as an energy efficiency measure for many industries [90,91]. They become however obsolete if no fuels are used. In 2016, industries in Germany produced 35.3 TWh of electricity, of which 86 % were fossil fuel-based [92]. This represents an industry self-supply with electricity of more than 15 %.

6. Conclusion

This work analyzed the techno-economic feasibility of two heat pump systems for the supply of process heat at high temperatures in large-scale applications. The two identified solutions were a reversed Brayton cycle using R-744 (CO_2) as working fluid and a cascade multi-stage compression cycle using R-718 (water) as working fluid in the high temperature section. It was found that equipment suitable for the operating conditions is available in oil and gas industries rather than in heat pump industries.

The analysis of the case studies indicated the possibility to economically supply process heat by electrically driven heat pumps at temperatures of up to 280 °C, while higher temperatures might be reached depending on the availability of suitable heat sources. The economic potential was highest for low electricity prices and it was emphasized that the acquisition and operation of own renewable electricity utilities becomes promising, especially for energy-intensive industries.

The comparison of the reversed Brayton cycle and the multi-stage steam compression cycle revealed competitive performances for both cycles in the considered applications, while the preferred choice is determined by the specific application. The reversed Brayton cycle is a simpler construction and is more promising in applications with large temperature glides. The reversed Brayton cycle had in both case studies a lower thermodynamic performance. Due to its simpler construction and lower investment costs, it had better economic performance in one case study. The cascade multi-stage cycle showed a higher flexibility with respect to the integration into given boundary conditions and had a higher thermodynamic performance. The increased flexibility is related to a more complex construction and accordingly higher investment cost, which might be compensated by the higher thermodynamic performance.

It was demonstrated that a heat pump-based process heat supply is technically feasible at temperatures of up to 300 °C to 400 °C. This enables supply of heat at higher temperatures and coverage of even more applications by electricity-based heat supply. This improves the overall energy efficiency of the plants and reduces the environmental impact from fossil fuel combustion. A large potential for implementing these technologies across many manufacturing industries was expected and possible other applications were pointed out.

The examples have furthermore highlighted, that the transition to heat pump-based process heat supply with an overall optimal energetic and economic performance requires a simultaneous and multi-disciplinary development including possible adjustments in the process, the design of the heat pump and the design of the components.

Declaration of Competing Interest

None.

Acknowledgements

This research publication is financially funded by The Danish Council for Strategic Research in Sustainable Energy and Environment, under the project title: “THERMCYC – Advanced thermodynamic cycles utilizing low-temperature heat sources” and by ELFORSK, the research and development fund of the Danish Energy Association, under the project (350-038) “Electrification of processes and technologies in the Danish industry“ as well as ”HighEFF-Centre for an Energy Efficient and Competitive Industry for the Future“, funded by the Research Council of Norway (FME grant 257632/E20).

Appendix

This section summarizes the state points of the numerical simulations as well as the component data for the economic evaluation.

Cascade multi-stage steam compression cycle (R-718)

Table A.1 summarizes the state points of the system as modelled for the alumina production case study. It includes the state points for both the top cycle and the two bottom heat pump cycles. The source and sink stream were assumed to be of constant heat capacity and not further specified. They are therefore omitted from the list. The source was cooled from 110 °C to 60 °C while the sink stream was heated from 140 °C to 280 °C. In the alumina production case study, no direct heating with liquid from the evaporator was required and the streams 26 and 27 were accordingly obsolete.

Table A.2 shows the state points of the cascade multi-stage system for the spray dryer case study including the bottom heat pump cycles and the heat source and sink streams.

Table A1
Thermodynamic modelling results of cascade multi-stage R-718 system for the alumina production case study.

State point	Mass flow rate kg/s	Pressure bar	Temp. °C	Spec. Enthalpy kJ/kg
Top cycle (R-718)				
1	–	2.3	125.0	525.1
2	16.9	2.3	125.0	2713.1
3	18.0	2.3	135.0	2734.8
4	16.9	7.4	302.2	3063.0
5	18.9	7.4	177.4	2790.1
6	16.1	7.4	177.4	2790.1
7	16.1	2.4	354.9	3140.8
8	18.3	2.4	231.3	2833.0
9	10.6	2.4	231.3	2833.0
10	10.6	6.8	397.3	3156.8
11	12.1	6.8	293.4	2823.7
12	12.1	6.8	283.4	1254.6
13	12.1	6.8	222.0	954.0
14	7.7	23.8	231.3	2833.0
15	7.7	23.8	221.3	949.6
16	19.8	23.8	221.3	952.3
17	19.8	23.8	167.4	708.5
18	2.8	7.4	177.4	2790.1
19	2.8	7.4	167.4	707.6
20	22.6	7.4	167.4	708.4
21	22.6	7.4	145.0	610.8
22	22.6	2.3	125.0	610.8
23	2.0	7.4	125.1	525.7
24	2.2	23.8	125.2	527.6
25	1.5	67.5	125.8	532.8
Bottom HP 1 (R-600)				
1	53.65	9.6	124.9	800.4
2	53.65	26.3	169.0	866.0
3	53.65	26.3	130.0	747.1
4	53.65	26.3	130.0	562.6
5	53.65	26.3	97.8	454.9
6	53.65	9.6	77.5	454.9
7	53.65	9.6	77.5	693.0
Bottom HP 2 (R-600)				
1	51.35	5.3	124.9	811.1
2	51.35	26.3	190.2	924.3
3	51.35	26.3	130.0	747.1
4	51.35	26.3	130.0	562.5
5	51.35	26.3	82.5	410.2
6	51.35	5.3	52.5	410.2
7	51.35	5.3	52.5	659.0

Table A2
Thermodynamic modelling results of cascade multi-stage R-718 system for the spray dryer case study.

State point	Mass flow rate kg/s	Pressure bar	Temp. °C	Spec. Enthalpy kJ/kg
Top cycle (R-718)				
1	–	0.7	90.0	377.0
2	2.36	0.7	90.0	2659.5
3	2.52	0.7	100.0	2679.8
4	2.36	2.3	257.1	2984.6
5	2.61	2.3	133.9	2733.2
6	1.94	2.3	133.9	2733.2
7	1.94	7.2	300.9	3060.8
8	2.16	7.2	176.0	2788.6
9	1.22	7.2	176.0	2788.6
10	1.22	21.8	344.0	3120.3
11	1.36	21.8	226.8	2830.9
12	1.36	21.8	216.8	928.6
13	1.36	21.8	166.4	704.3
14	0.94	7.2	176.0	2788.6
15	0.94	7.2	166.0	701.6
16	2.30	7.2	166.0	703.2
17	2.30	7.2	123.9	520.8
18	0.67	2.3	133.9	2733.2
19	0.67	2.3	123.9	520.5
20	2.98	2.3	123.9	520.7
21	2.98	2.3	90.0	377.2
22	2.98	0.7	90.0	377.2
23	0.25	2.3	90.0	377.2
24	0.22	7.2	90.1	377.8
25	0.14	21.8	90.2	379.5
26	13.34	0.7	90.0	377.2
27	13.34	0.7	71.8	300.6
Bottom HP 1 (R-600)				
1	4.39	2.3	89.0	742.7
2	4.39	13.7	156.1	864.3
3	4.39	13.7	95.0	714.6
4	4.39	13.7	95.0	446.2
5	4.39	13.7	48.8	319.4
6	4.39	2.3	23.3	319.4
7	4.39	2.3	23.3	617.7
Bottom HP 2 (R-600)				
1	10.1	1.6	89.0	744.6
2	10.1	13.7	168.3	894.3
3	10.1	13.7	95.0	714.6
4	10.1	13.7	95.0	446.1
5	10.1	13.7	42.0	302.0
6	10.1	1.6	12.4	302.0
7	10.1	1.6	12.4	602.2
Heat sink stream (Moist air, humidity at inlet: 6.43 g/kg)				
Si1	54.9	1.0	64.3	81.5
Si2	54.9	1.0	82.5	100.0
Si3	54.9	1.0	90.1	107.8
Si4	54.9	1.0	116.7	135.0
Si5	54.9	1.0	124.1	142.6
Si6	54.9	1.0	158.9	178.4
Si7	54.9	1.0	164.3	183.9
Si8	54.9	1.0	210.0	231.2
Heat source stream (Moist air, humidity at inlet: 28.88 g/kg)				
So1	64.3	1.0	50.0	125.2
So2	64.3	1.0	30.8	104.8
So3	64.3	1.0	19.9	57.7

Reversed Brayton cycle (R-744)

Table A.3 shows the state points for the reversed Brayton cycle for the alumina production case study. The source and sink stream were assumed to be of constant heat capacity and not further specified. They were therefore omitted from the table. The source was cooled from 110 °C to 60 °C while the sink stream was heated from 140 °C to 280 °C.

Table A.4 shows the state points of the reversed Brayton cycle for the spray dryer case including the heat source and sink streams.

Table A3
Thermodynamic modelling results of the reversed Brayton cycle for the alumina production case study.

State point	Mass flow rate kg/s	Pressure bar	Temp. °C	Spec. Enthalpy kJ/kg
Reversed Brayton cycle (R-744)				
1	278.7	40.7	139.9	83.6
2	278.7	140.0	290.0	220.9
3	278.7	140.0	147.5	41.5
4	278.7	140.0	121.2	1.6
5	278.7	40.7	29.1	−41.8
6	278.7	40.7	102.5	43.7

Table A4
Thermodynamic modelling results of the reversed Brayton cycle for the spray dryer case study.

State point	Mass flow rate kg/s	Pressure bar	Temp. °C	Spec. Enthalpy kJ/kg
Reversed Brayton cycle (R-744)				
1	64.3	25.2	100.6	51.6
2	64.3	72.0	217.5	155.4
3	64.3	72.0	106.6	27.5
4	64.3	72.0	63.6	−31.9
5	64.3	25.2	−6.8	−64.2
6	64.3	25.2	42.3	−7.9
Heat sink stream (Moist air, humidity at inlet: 6.43 g/kg)				
Si1	54.9	1.0	64.3	81.5
Si2	54.9	1.0	210.0	231.2
Heat source stream (Moist air, humidity at inlet: 28.88 g/kg)				
So1	64.3	1.0	50.0	125.2
So2	64.3	1.0	23.0	68.9

References

[1] Kost C, Shammugam S, Jülch V, Nguyen H-T, Schlegl T, Henning H-M, et al. Levelized Cost of Electricity - Renewable Energy Technologies 2018. https://www.ise.fraunhofer.de/en/publications/studies/cost-of-electricity.html (accessed January 14, 2019).

[2] Schlesinger M, Hofer P, Kemmler A, Kirchner A, Koziel S, Ley A, et al. Development of energy markets - Energy reference forecast [In German: Entwicklung der Energiemärkte – Energiereferenzprognose]. Prognos 2014:Projekt Nr. 57/12. https://www.bmwi.de/Redaktion/DE/Publikationen/Studien/entwicklung-der-energiemaerkte-energiereferenzprognose-endbericht.pdf?_blob=publicationFile&v=7 (accessed January 15, 2019).

[3] European Commission. A Roadmap for moving to a competitive low carbon economy in 2050 2011. https://ec.europa.eu/clima/policies/strategies/2050_en#tab-0-1 (accessed January 15, 2019).

[4] Danish Ministry of Energy Utilities and Climate. Energistrategi 2050 - fra kul, olie og gas til grøn energi 2011:65. https://www.regeringen.dk/tidligere-publikationer/energistrategi-2050-fra-kul-olie-og-gas-til-groen-energi/ (accessed January 15, 2019).

[5] Sustainable Development Solutions Network (SDSN), Institute for Sustainable Development and International Relations (IDDRI). Deep Decarbonization Pathways Project – Pathways to deep decarbonization 2015:1–58. http://deepdecarbonization.org/wp-content/uploads/2016/03/DDPP_2015_REPORT.pdf%0Apapers2://publication/uuid/E7622E05-580D-4FEC-9AB7-DFE70AA5D572.

[6] Bataille C, Åhman M, Neuhoff K, Nilsson LJ, Fischedick M, Lechtenböhmer S, et al. A review of technology and policy deep decarbonization pathway options for making energy-intensive industry production consistent with the Paris agreement. J Clean Prod 2018;187:960–73. https://doi.org/10.1016/j.jclepro.2018.03.107.

[7] UNFCCC Paris Agreement. Conf Parties Its Twenty-First. Sess 2015;32.

[8] McMillan C, Boardman R, Mckellar M, Sabharwall P, Ruth M, Bragg-sitton S, et al. Generation and use of thermal energy in the U. S. Industrial sector and opportunities to reduce its carbon emissions. NREL/TP-6A50-66763 2016.

[9] Eurostat. Energy statistics – supply, transformation and consumption, 2017.

[10] Wolf S, Blesl M. Model-based quantification of the contribution of industrial heat pumps to the European climate change mitigation strategy. ECEEE Ind Summer Study Proc 2016:477–87.

[11] Philibert C. Renewable Energy for Industry – From green energy to green materials and fuels. Int Energy Agency 2017:72 (accessed January 15, 2019).

[12] Esser A, Sensfuss F. Final report - Evaluation of primary energy factor calculation options for electricity 2016:121. https://ec.europa.eu/energy/sites/ener/files/documents/final_report_pef_eed.pdf (accessed January 15, 2019).

[13] Elmegaard B, Zühlsdorf B, Reinholdt L, Bantle M, editors. International Workshop on High Temperature Heat Pumps. B Present Int Work High Temp Heat Pumps 2017:176. http://orbit.dtu.dk/en/publications/book-of-presentations-of-the-international-workshop-on-high-temperature-heat-pumps (0351887a-6b82-4b3d-aae5-19181db64891).html (accessed January 15, 2019).

[14] Arpagaus C, Bless F, Uhlmann M, Schiffmann J, Bertsch SS. High temperature heat pumps: market overview, state of the art, research status, refrigerants, and application potentials. Energy 2018:152. https://doi.org/10.1016/j.energy.2018.03.166.

[15] Wolf S, Fahl U, Blesl M, Voss A, Jakobs R. Forschungsbericht – Analyse des Potenzials von Industriewärmepumpen in Deutschland 2014:150. http://www.ier.uni-stuttgart.de/publikationen/veroeffentlichungen/forschungsberichte/downloads/141216_Abschlussbericht_FKZ_0327514A.pdf (accessed January 15, 2019).

[16] Pehnt M, Bödeker J, Arens M, Jochem E, Idrissova F. Die Nutzung industrieller Abwärme – technisch-wirtschaftliche Potentiale und energiepolitische Umsetzung 2010:49. https://www.ifeu.de/wp-content/uploads/Nutzung_industrieller_Abwaerme.pdf (accessed January 15, 2019).

[17] Thekdi A, Nimbalkar SU. Industrial waste heat recovery: potential applications. Avail Technol Crosscutting R&D Opport 2014. https://doi.org/10.2172/1185778.

[18] Kang DH, Na S-I, Kim MS. Recent researches on steam generation heat pump system. Int J Air-Condition Refrig 2017. https://doi.org/10.1142/S2010132517300051.

[19] Bless F, Arpagaus C, Bertsch SS, Schiffmann J. Theoretical analysis of steam generation methods – energy, CO2emission, and cost analysis. Energy 2017;129:114–21. https://doi.org/10.1016/j.energy.2017.04.088.

[20] Kaida T, Sakuraba I, Hashimoto K, Hasegawa H. Experimental performance evaluation of heat pump-based steam supply system. IOP Conf Ser: Mater Sci Eng 2015;90:012076. https://doi.org/10.1088/1757-899X/90/1/012076.

[21] Lee G, Lee B, Cho J, Ra H-S, Baik Y, Shin H-K, et al. Development of steam

generation heat pump through refrigerant replacement approach. Rotterdam: 12th IEA Heat Pump Conf.; 2017. p. 1–10. Paper ID: P.3.3.2.
[22] Meroni A, Zühlsdorf B, Elmegaard B, Haglind F. Design of centrifugal compressors for heat pump systems. Appl Energy 2018;232:139–56. https://doi.org/10.1016/j.apenergy.2018.09.210.
[23] Bühler Fabian, Zühlsdorf Benjamin, Nguyen Tuong-Van, Elmegaard Brian. A comparative assessment of electrification strategies for industrial sites: Case of milk powder production. Appl Energy 2019;250:1383–401. https://doi.org/10.1016/j.apenergy.2019.05.071.
[24] Madsbøll H, Weel M, Kolstrup A. Development of a water vapor compressor for high temperature heat pump applications. Yokohama, Japan: Proc. Int. Congr. Refrig.; 2015. p. 845.
[25] Bantle M, Tolstorebrov I, Eikevik TM. Possibility for mechanical vapor re-compressrion for steam based drying processes. Proc. 1st Nord. Balt. Dry. Conf. 2015.
[26] Bantle M. Turbo-compressors : Prototype tests of mechanical vapour re-compression for steam driers. Rotterdam: Proc. 12th IEA Heat Pump Conf.; 2017. Paper ID: O.3.5.4.
[27] Bantle M, Schlemminger C, Tolstorebrov I, Ahrens M, Evenmo K. Performance evaluation of two stage mechanical vapour recompression with turbo-compressors. Proc. 13th IIR Gustav Lorentzen Conf. Nat. Refrig.; 2018. p. 1157. 10.18462/iir.gl.2018.1157.
[28] Zühlsdorf B, Schlemminger C, Bantle M, Evenmo K, Elmegaard B. Design Recommendations for R718 Heat Pumps in High Temperature Applications. Valencia: Proc. 13th IIR Gustav Lorentzen Conf. Nat. Refrig.; 2018. 10.18462/iir.gl.2018.1367.
[29] Chamoun M, Rulliere R, Haberschill P, Peureux J-L. Experimental and numerical investigations of a new high temperature heat pump for industrial heat recovery using water as refrigerant. Int J Refrig 2014;44:177–88. https://doi.org/10.1016/j.ijrefrig.2014.04.019.
[30] Chamoun M, Rulliere R, Haberschill P, Peureux J-L. Experimental investigation of a new high temperature heat pump using water as refrigerant for industrial heat recovery. Purdue: Proc. Int. Refrig. Air Cond. Conf.; 2012. Paper ID 2108.
[31] De Larminat P, Arnou D, Le Sausse P, Clunet F, Peureux J-L. A High Temperature Heat Pump Using Water Vapor as Working Fluid. Hangzhou, China: Proc. 11th IIR Gustav Lorentzen Conf.; 2014. Paper No.: GL-55.
[32] Šarevski MN, Šarevski VN. Thermal characteristics of high-temperature R718 heat pumps with turbo compressor thermal vapor recompression. Appl Therm Eng 2017;117:355–65. https://doi.org/10.1016/j.applthermaleng.2017.02.035.
[33] Šarevski MN, Šarevski VN. Characteristics of water vapor turbocompressors applied in refrigeration and heat pump systems. Int J Refrig 2012;35:1484–96. https://doi.org/10.1016/j.ijrefrig.2012.03.014.
[34] Zühlsdorf B, Bühler F, Mancini R, Cignitti S, Elmegaard B. High Temperature Heat Pump Integration using Zeotropic Working Fluids for Spray Drying Facilities. Rotterdam: 12th IEA Heat pump Conf.; 2017. p. 1–11.
[35] Angelino G, Invernizzi C. Prospects for real-gas reversed Brayton cycle heat pumps. Int J Refrig 1995;18:272–80. https://doi.org/10.1016/0140-7007(95)00005-V.
[36] Fu C, Gundersen T. A novel sensible heat pump scheme for industrial heat recovery. Ind Eng Chem Res 2016;55:967–77. https://doi.org/10.1021/acs.iecr.5b02417.
[37] Aga V, Conte E, Carroni R, Burcker B, Ramond M. Supercritical CO2-Based Heat Pump Cycle for Electrical Energy Storage for Utility Scale Dispatchable Renewable Energy Power Plants. San Antonio Texas: 5th Int. Supercrit. CO2 Power Cycles Symp; 2016.
[38] Malpiece D, Montressor P, Aga VK, Nikulshyna V. Electrical energy storage and discharge system. EP 2 942 492 Al 2015.
[39] Aga V, Conte E. Electrical energy storage and discharge system. EP 3 054 155 B1 2017.
[40] Bamigbetan O, Eikevik TM, Nekså P, Bantle M, Schlemminger C. Theoretical analysis of suitable fluids for high temperature heat pumps up to 125 °C heat delivery. Int J Refrig 2018;92:185–95. https://doi.org/10.1016/j.ijrefrig.2018.05.017.
[41] Zühlsdorf B, Jensen JK, Elmegaard B. Heat pump working fluid selection – economic and thermodynamic comparison of criteria and boundary conditions. Int J Refrig 2019;98:500–13. https://doi.org/10.1016/j.ijrefrig.2018.11.034.
[42] Zühlsdorf B, Jensen JK, Elmegaard B. Numerical models for the design and analysis of heat pumps with zeotropic mixtures, Rev01 2018. doi: https://doi.org/10.11583/DTU.6825443.
[43] Lorenz H. Beiträge zur Beurteilung von Kühlmaschinen. Zeitschrift Des VDI 1894;38:62–8.
[44] Bejan A, Tsatsaronis G, Moran M. Thermal Design and Optimization 1996. https://doi.org/10.1016/S0140-7007(97)87632-3.
[45] VDI-Gesellschaft Verfahrenstechnik und Chemieingenieurwesen. VDI Heat Atlas. Berlin, Heidelberg: Springer Berlin Heidelberg; 2010.
[46] Turton R, Bailie RC, Whiting WB, Shaeiwitz JA, Bhattacharyya D. Analysis Synthesis, and Design of Chemical Processes. Fourth Pearson Education, Inc.; 2012.
[47] Ulrich GD, Vasudevan PT. Chemical Engineering Process Design and Economics: A Practical Guide. Durham, New Hampshire: Process Publishing Company; 2004.
[48] Towler G, Sinnott R. Chemical Engineering Design - Principles, Practice and Economics of Plant and Process Design. 2nd ed. Elsevier Ltd.; 2012. 10.1016/C2009-0-61216-2.
[49] Eurostat. Energy statistics - supply, transformation and consumption 2017. https://ec.europa.eu/eurostat/web/energy/data/database?p_p_id=NavTreeportletprod_WAR_NavTreeportletprod_INSTANCE_QAMy7Pe6HwI1&p_p_lifecycle=0&p_p_state=normal&p_p_mode=view&p_p_col_id=column-2&p_p_col_count=1 (accessed January 14, 2019).
[50] Danish Energy Agency. Finding your cheapest way to a low carbon future: The Danish Levelized Cost of Energy Calculator 2017. https://ens.dk/en/our-responsibilities/global-cooperation/levelized-cost-energy-calculator (accessed January 15, 2019).
[51] Kost C, Shammugam S, Jülch V, Nguyen H-T, Schlegl T, Henning H-M, et al. Level Cost Electricity – Renew Energy Technol 2018.
[52] Statnett. Long Term Market Analysis, the Nordic Region and Europe 2016. https://www.statnett.no/globalassets/for-aktorer-i-kraftsystemet/planer-og-analyser/long-term-market-analysis-the-nordic-region-and-europe-2016-2040.pdf (accessed January 15, 2019).
[53] The Norwegian Tax Administration. Electrical power tax - The Norwegian Tax Administration 2018. https://www.skatteetaten.no/en/business-and-organisation/vat-and-duties/excise-duties/about-the-excise-duties/electrical-power-tax/ (accessed January 15, 2019).
[54] PwC (Price Waterhouse Coopers). Overview for the accounting and reimburesment of taxes [In Danish: Samlet overblik over afregning og godtgørelse af afgifter] 2018. https://www.pwc.dk/da/publikationer/2019/01/afgiftsvejledning.html.
[55] Danish Energy Agency. Baseline projection 2018 [Basisfremskrivning 2018] 2018. https://ens.dk/sites/ens.dk/files/Analyser/basisfremskrivning_2018.pdf (accessed January 15, 2019).
[56] Danish Energy Agency. Technology Data for Individual Heating Plants 2016. https://ens.dk/en/our-services/projections-and-models/technology-data/technology-data-individual-heating-plants (accessed January 15, 2019).
[57] Danish Energy Agency. Biogas in Denmark- status, barriers and perspectives [In Danish: Biogas i Danmark-status, barrierer og perspektiver] 2014. https://ens.dk/sites/ens.dk/files/Bioenergi/biogas_i_danmark_-_analyse_2014-final.pdf (accessed January 15, 2019).
[58] Danish Energy Agency. Socioeconomic calculation basis for energy prices and emissions [In Danish: Samfundsøkonomiske beregningsforudsætninger for energipriser og emissioner] 2017:25. https://ens.dk/sites/ens.dk/files/Analyser/samfundsoekonomiske_beregningsforudsaetninger_2017.pdf (accessed January 15, 2019).
[59] Gomez DR, Watterson JD, Americano BB, Ha C, Marland G, Matsika E, et al. 2006 IPCC Guidelines for National Greenhouse Gas Inventories. Volume 2: Energy. Chapter 2: Stationary Combustion. 2007.
[60] Naegler T, Simon S, Klein M, Gils HC. Quantification of the European industrial heat demand by branch and temperature level. Int J Energy Res 2015;39:2019–30. https://doi.org/10.1002/er.3436.
[61] Rehfeldt M, Fleiter T, Toro F. A bottom-up estimation of the heating and cooling demand in European industry. Energy Effic 2018;11:1057–82. https://doi.org/10.1007/s12053-017-9571-y.
[62] McKenna RC, Norman JB. Spatial modelling of industrial heat loads and recovery potentials in the UK. Energy Policy 2010;38:5878–91. https://doi.org/10.1016/j.enpol.2010.05.042.
[63] Hammond GP, Norman JB. Heat recovery opportunities in UK industry. Appl Energy 2014;116:387–97. https://doi.org/10.1016/j.apenergy.2013.11.008.
[64] Fleiter T, Fehrenbach D, Worrell E, Eichhammer W. Energy efficiency in the German pulp and paper industry – a model-based assessment of saving potentials. Energy 2012;40:84–99. https://doi.org/10.1016/j.energy.2012.02.025.
[65] Bengtsson C, Nordman R, Berntsson T. Utilization of excess heat in the pulp and paper industry – a case study of technical and economic opportunities. Appl Therm Eng 2002;22:1069–81. https://doi.org/10.1016/S1359-4311(02)00017-0.
[66] Norgate TE, Jahanshahi S, Rankin WJ. Assessing the environmental impact of metal production processes. J Clean Prod 2007;15:838–48. https://doi.org/10.1016/j.jclepro.2006.06.018.
[67] Donaldson DJPE. Perspective of Bayer Process Energy. Light Met 2013:711–5.
[68] Metson J. Production of Alumina Fundam. Alum. Metall. Prod. Process. Appl., Woodhead Publishing Limited; 2011. p. 23–48. 10.1016/B978-1-84569-654-2.50002-X.
[69] Wischnewski R, Maues Jr CDA, Moraes ELS, Monteiro AB. Alunorte global energy efficiency. Light Met 2011:179–84.
[70] Kelly R, Edwards M, Deboer D, Mcintosh P. New technology for digestion of bauxites. Light Met 2006:371–6.
[71] Songqing G, Zhonglin Y. Preheaters and digesters in the bayer digestion process. Light Met 2004:356–61.
[72] Scarsella AA, Noack S, Gasafi E, Klett C, Koschnick A. Energy in alumina refining: setting new limits. Light Met 2015;2015:131–6. https://doi.org/10.1002/9781119093435.ch24.
[73] Ilievski D, Hay P, Mills G, Bauer G, Bayer Ünal A. Calcination waste heat recovery. Proc. 8th Int. Alumina Qual. Work; 2008. p. 125–9.
[74] Singh RP, Heldman DR. Introduction to Food Engineering. 5th ed. Elsevier Inc.; 2014.
[75] Bühler F, Nguyen T-V, Jensen JK, Holm FM, Elmegaard B. Energy, exergy and advanced exergy analysis of a milk processing factory. Energy 2018;162:576–92. https://doi.org/10.1016/j.energy.2018.08.029.
[76] European Commission. Reference document on best available techniques in the production of polymers 2007:314. http://eippcb.jrc.ec.europa.eu/reference/BREF/pol_bref_0807.pdf (accessed January 15, 2019).
[77] Fleiter T, Schlomann B, Eichhammer W. Energy use and CO2-emissions of industrial process technologies - saving potentials, barriers and instruments [In German: Energieverbrauch und CO2 -Emissionen industrieller Prozesstechnologien – Einsparpotenziale, Hemmnisse und Instrumente]. Stuttgart: Fraunhofer Verlag; 2013.
[78] Dumont Y, Aujollet P, Ferrasse JH. Use of a heat pump to supply energy to the iodine-sulphur thermochemical cycle for hydrogen production. Int J Chem React Eng 2010:8.
[79] Almahdi M, Dincer I, Rosen MA. A new integrated heat pump option for heat upgrading in Cu-Cl cycle for hydrogen production. Comput Chem Eng 2017;106:122–32. https://doi.org/10.1016/j.compchemeng.2017.05.009.
[80] Nemet A, Klemeš JJ, Varbanov PS, Mantelli V. Heat Integration retrofit analysis an oil refinery case study by Retrofit Tracing Grid Diagram. Front Chem Sci Eng 2015;9:163–82. https://doi.org/10.1007/s11705-015-1520-8.
[81] Norsk Hydro ASA. Rolling processes [In German: Walzprozesse] 2016. https://www.hydro.com/de/hydro-in-deutschland/Walzprodukte/Walzprozesse/ (accessed January 15, 2019).
[82] Utlu Z, Hepbaşlı A. Exergoeconomic analysis of energy utilization of drying process in a ceramic production. Appl Therm Eng 2014;70:748–62. https://doi.org/10.

1016/j.applthermaleng.2014.05.070.
[83] Rubio MC, Martínez G, Baena L, Moreno F. Warm mix asphalt: an overview. J Clean Prod 2012;24:76–84. https://doi.org/10.1016/j.jclepro.2011.11.053.
[84] Utlu Z, Hepbasli A, Turan M. Performance analysis and assessment of an industrial dryer in ceramic production. Dry Technol 2011;29:1792–813. https://doi.org/10.1080/07373937.2011.602921.
[85] European Comission. Energy saving in the brick and tile industry 1998. https://publications.europa.eu/en/publication-detail/-/publication/0d5e9ce7-0ebd-4186-b1b1-4a1a9f942cdb.
[86] Mujumdar AS. Handbook of Industrial Drying. 4th ed. CRC Press; 2014.
[87] Jensen AS. Drying in Superheated Steam under Pressure. NDC, Helsinki: Fifth Nord. Dry. Conf; 2011.
[88] Ma T, Wang Q, Chu W, Li X, Chen Y. Experimental investigation on SCO 2 -water heat transfer characteristics in a printed circuit heat exchanger with straight channels. Int J Heat Mass Transf 2017;113:184–94. https://doi.org/10.1016/j.ijheatmasstransfer.2017.05.059.
[89] Henrickson L. The need for energy efficiency in bayer refining. Light Met 2010:691–6.
[90] Saygin D, Patel M, Tam C, Gielen D. Chemical and Petrochemical sector. Potential of best practice technology and other measures for improving energy efficiency. IEA Inf Pap OECD/IEA 2009:1–60.
[91] Suhr M, Klein G, Kourti I, Rodrigo Gonzalo M, Giner Santonja G, Roudier S, et al. Best Available Techniques (BAT) reference document for the production of pulp Paper Board. JRC Sci Policy Rep 2015. https://doi.org/10.2791/370629.
[92] AG Energiebilanzen e.V. Auswertungstabellen zur Energiebilanz Deutschland. 1990 bis 2017 (Stand Juli 2018) 2018. https://www.ag-energiebilanzen.de/10-0-auswertungstabellen.html (accessed January 15, 2019).